Check for updates

EurJIC
European Journal of Inorganic Chemistry

Research Article
doi.org/10.1002/ejic.202300495

Chemistry Europe
European Chemical Societies Publishing

www.eurjic.org

VIP *Very Important Paper*

Special Collection

Are Monophospha(III)amidines and -guanidines with Ionizable Hydrogens Tautomeric? Towards a Deeper Understanding of Two Related Hetero-element Functional Groups

Jason D. Masuda,[a] Leila Mokhtabad Amrei,[b] and René T. Boeré*[b]

Professor Rainer Streubel has been a leader in many areas of low-coordinate phosphorus chemistry. He has maintained an astonishingly wide network of national and international collaborators. We have benefited enormously from his outstanding organizational energy and warm Rhineland hospitality.

This paper presents definitive structural evidence for *N*,*P*(III)-monophosphaamidines in P=C and N=C isomeric forms from a combination of new syntheses, single-crystal X-ray diffraction (SC-XRD), solid-state NMR and FTIR. Evidence is also provided for *C*-amino-(σ^2,λ^3)-phosphaalkene and *C*-(σ^3,λ^3)-phosphinoimine tautomerism in solution using multi-nuclear NMR methods. Synthesis and SC-XRD structure determination of a trisubstituted *N*,*N*′,*P*(III)-monophosphaguanidine is presented, the first structure of a phospha(III)guanidine with two ionizable H atoms. The structural evidence is convincing for an N=C geometry, resulting in both N–H and P–H in the molecule. A detailed computational investigation using DFT methods is presented, with the goal of understanding the tautomeric structure preferences both at the fundamental level (parent molecules with all substituents on the heteroatoms being hydrogen) and using the full structures containing the very bulky 2,6-diisopropylphenyl (Dipp) substituents employed in this study. Arguments are espoused for treating phospha(III)amidines and -guanidines as new types of functional groups, similar to but distinct from the familiar organic analogues. Limited reactivity studies and a voltammetry study of one phospha(III)amidine are included with the supporting information.

Introduction

Interest in multiple-bonding and associated effects involving the heavier main group elements continues to expand as we approach the 60th anniversary of the first report of a C,P multiple bond.[1,2] Maturity of the field is attested by the current focus on applications in, for example, polymers of *p*-block elements,[2i,3] π-conjugated low-coordinate phosphorus compounds,[4] and their use in organic electronics.[5] Recently, there has been an explosion of relevant literature with new preparative methods and exciting products, with new structure types and a growing body of structural information,[6–16] chemistry towards which Prof. Rainer Streubel has made significant contributions over decades.[17]

Within the field of carbon-phosphorus multiple bonds, amino- and diaminophosphaalkenes (monophospha(III)amidines **I** and monophospha(III)guanidines **II**, Scheme 1)[19] are well recognized entities characterized by so-called *inverse polarization* by comparison to parent or carbon-substituted phosphaalkenes.[20] Some of the earliest-reported phosphaalkenes belong to these classes, including **A–C** (Scheme 1) amongst the earliest to be structurally characterized.[21] But it would be a mistake to think that these are the only, or even the dominant structure classes. As drawn, structures **I** and **II** draw attention to the possibility of replacing *either* amino *or* imino nitrogens in the organic functional groups by P(III). There are now structurally verified examples of most possibilities; space prevents an exhaustive listing, so one illustrative exemplar is provided for each case in Scheme 1 along with its CSD refcode. Both *C*-amino-(σ^2,λ^3)-phosphaalkene (P=C, illustrated by **B**)[21i] and *C*-(σ^3,λ^3)-phosphinoimine (N=C, illustrated by **D**)[22] isomers of monophospha(III)amidines have numerous exemplars. Diphospha(III)amidines, by contrast, are rare but do exist as illustrated by **E**.[23] **C** is an early example of an acyclic monophospha(III)guanidine (P=C) isomer,[21g,h] which remain relatively sparse, in contrast to the very numerous cyclic variants illustrated by **A**; in modern parlance, **A** is recognized as an N-heterocyclic-carbene (NHC) adduct of a phosphinidene, as

[a] *Prof. Dr. J. D. Masuda*
Department of Chemistry
Saint Mary's University
Halifax, Nova Scotia, B3H 3C3 (Canada)

[b] *Dr. L. Mokhtabad Amrei, Prof. Dr. R. T. Boeré*
Department of Chemistry and Biochemistry and The Canadian Centre for Advanced Fluorine Technologies
University of Lethbridge
Lethbridge, Alberta, T1K 3M4 (Canada)
E-mail: boere@uleth.ca

Supporting information for this article is available on the WWW under https://doi.org/10.1002/ejic.202300495

Part of the celebratory collection for Rainer Streubel.

Research Article
doi.org/10.1002/ejic.202300495

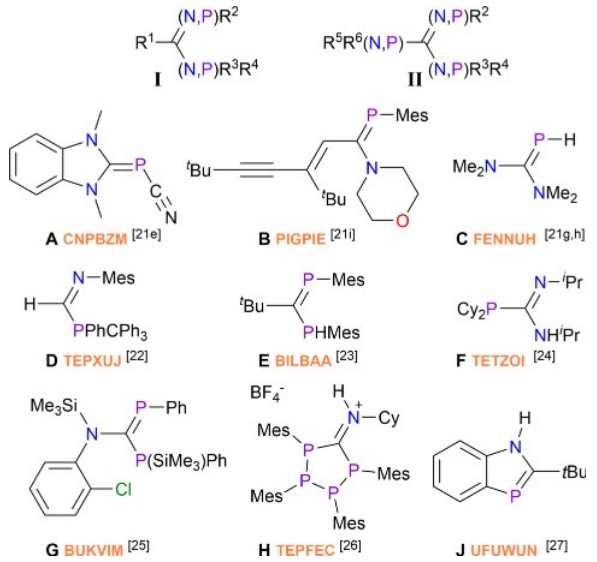

Scheme 1. Relevant structures with CSD refcodes (the Cambridge Structural Database, release 2023.1.0).[18]

made famous by Arduengo.[28,29] The NHC interaction with both elemental pnictogens and pnictinidenes has grown into a massive field of research in its own right.[30,31] Confusingly, both types **B** and **A**/**C** are very often called 'aminophosphaalkenes' without distinction, especially when inverse polarization of the P=C bond is being emphasized.[32] Not to be outdone, however, (N=C) isomeric monophospha(III)guanidines have grown to significance as particularly electron-rich R_2P- backbone-substituted amidinates in coordination chemistry.[33,34] The phospha(III)guanidine **F** exemplifies one such pro-ligand.[24] Diphospha(III)guanidines are surprisingly common in the (P=C) isomeric form, illustrated by **G**,[25] but rare as (N=C). A structure of a protonated derivative of the latter, **H**, illustrates the type, but the parent base is also well characterized.[26] There are no genuine triphospha(III)guanidines, the structural framework of which exists either as Ph_3P ylides of bis(diphenylphosphino)methanides[35] or as metal-coordinated tris(diphenylphosphino)methanide ions.[36] One cyclic species that contains the triphospha(III)guanidine framework has been reported only in the form of a CSD Private Communication (refcode: NURZAB).[37] Just as for the organic functional group analogues, there is an extensive chemistry of cyclic phospha(III)amidines, e.g. as illustrated by **J**,[27] which will not be considered here.

Historically, the majority of phospha(III)amidines and phospha(III)guanidines that have been prepared and characterized have been fully substituted, i.e. 3° or 5° structures, respectively, as reflected in most of the examples in Scheme 1. Surprisingly little is still known about the chemistry of examples with ionizable substituents at N, P or both (in practice, either an H atom or a trimethylsilyl group). An early communication by Niecke in 1995 reported on NH_2 and $NHSiMe_3$ derivatives of **I** (P=C isomer, $R^1 = CH_3$ or Ph; R^2 = Ph, Mes), some of which are structurally characterized,[38,39] but nothing further has been reported about these interesting examples. Early reports from Issleib of 2° NH and $NSiMe_3$ derivatives of **I** claimed both (P=C) and (N=C) isomeric forms, based on limited NMR data.[21b] Recently Song et al. reported on the first 2° monophosphaformamidines which are claimed to be (P=C) isomers, also on NMR spectroscopic evidence.[40] Li *et al.*, by contrast, claimed the (N=C) isomer for a 2° derivative of **I** with $R^1 = {}^t$Bu.[41] Structurally confirmed (N=C) isomers of **I**, also with $R^1 = {}^t$Bu, prepared by a versatile new synthetic approach, have been reported by Lammertsma (CSD refcodes: XOPBAH; XOPCOW).[16] All of these 2° derivatives were targeted specifically as proligands for 'phospha(III)amidinate' complexes by direct analogy to the hugely important amidinate/guanidinate coordination chemistry.[42] Neutral amidines and guanidines are themselves important ligands,[42] and hence 3° phospha(III)amidines in the (N=C) isomeric form with PR_2 substituents have also been exploited in coordination chemistry, chelating via the imino N and P(III) lone pairs.[43–46] In particularly elegant work, Waterman showed that N,P-disubstituted phospha(III)amidines can be prepared by insertion into a transition metal phosphide bond; 1° phosphido producing terminal (κN)-amidinates, while 2° phosphido lead to chelating amidinates with backbone R_2P substituents.[22] Moreover, some phosphido complexes can catalyze the hydrophosphination of carbodiimides to afford monophospha(III)guanidines.[2h,47] This follows earlier work especially by Weber on metallaphosphaalkenes with both dative and covalent bonds to metals.[48]

Whereas the focus of most previous work has either been on 3° derivatives of **I** (or 5° of **II**), i.e. on phosphaalkenes exhibiting *inverse polarization*, or on deprotonated anionic ligands for coordination chemistry, a functional group approach has not been in vogue in low-valent phosphorus chemistry. In particular, little seems to be known about tautomerism and the associated facile interconversions that are so typical of the organic chemistry of amidines and guanidines, and which contribute to their extensive chemical reactivity.[49] To do so is, certainly, less of a focus on 'phosphorus the carbon mimic', and more of a periodic group analogy for replacing N=C double and partial double bonds with P=C. This should not be done naïvely; rather, with full recognition of the differences in element characteristics attending the replacements. To that end, we deliberately synthesized monophospha(III)amidines and a monophospha(III)guanidine with atom-equivalent structures, namely the benzamidine derivatives **1a** with bis(*N*,*P*)-2,6-diisopropylphenyl (Dipp) and R = $CH_3C_6H_4$− and **1b** (R = $CH_3OC_6H_4$−) and **4** with tris(*N*,*N*,*P*)-Dipp (Scheme 2). The structures of the former two have been reported previously[50,51] The analogous all-nitrogen compounds had been thoroughly (structurally and spectroscopically) characterized.[52,53]

Here we present a detailed structural, spectroscopic and computational investigation of the isomerism of the species in Scheme 2, with a focus on understanding them from a functional group perspective. New low-temperature X-ray structures of **1a,b** and the first of **2** are reported, in order to confirm the isomeric preferences. After a great deal of effort, an original claim of Issleib et al. that **3** occurs as the (N=C) isomer could be confirmed.[21b] The monophospha(III)guanidine **4** was also

Research Article
doi.org/10.1002/ejic.202300495

Chemistry Europe
European Chemical Societies Publishing

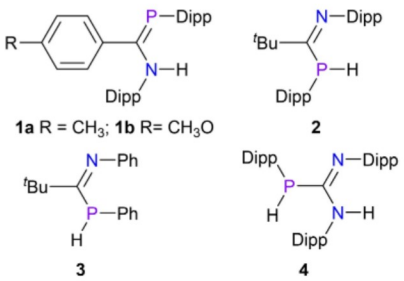

Scheme 2. Compounds described in this work.

synthesized and structurally characterized to show that it too is the (N=C) isomer.[54,55] The crystal structures of **2** and **3** indicate unambiguously the presence of *C*-(σ^3,λ^3)-phosphinoimines (N=C isomeric form). By contrast, **1a,b** seem to crystallize in the *C*-amino-(σ^2,λ^3)-phosphaalkenes (P=C form); and yet highly purified crystalline samples show up to four isomers after dissolution in NMR solvents under stringent conditions (purified solvents; tubes sealed under vacuum). The relative proportions of the isomers differ with solvent polarity, confirming an *E*/*Z* isomerism (not observed for **2** or **4**). ^{1}H/^{2}D exchange with NMR solvent and an EXSY NMR experiment support the notion of a solution equilibrium between P=C and N=C tautomers. Solid state ^{31}P NMR provides strong confirmation that small amounts of tautomeric *C*-(σ^3,λ^3)-phosphinoimines (N=C form) are present in the bulk crystalline samples. For this reason, considerable effort was taken to optimizing the crystal structure refinements by making use of newly developed methods employing custom aspherical atomic scattering factors.[56] These methods are particularly suited to locate H-atom electron density and accurately place the proton nuclei, which is crucial to the question of tautomer co-crystallization.[57] The results of our investigations are interpreted in the light of extensive hybrid DFT molecular orbital calculations and make use of a fragment orbital analysis to provide a rationale for the observed structural preferences. Some limited reactivity – beyond coordination chemistry – and a voltammetric study of **1a** round out this work.

Results and Discussion

Isomers and Conformers

Discussion of amidines and phospha(III)amidines, either in the solid state or in solution, requires a detailed consideration of possible isomers (Scheme 3).[58] Replacement of one of the nitrogen atoms of an amidine conceptually leads to two different structures: if the double bond is between P and C, a *C-amino-*(σ^2,λ^3)*-phosphaalkene* is formed; if between N and C, a *C-*(σ^3,λ^3)*-phosphinoimine*. In *N,P*-disubstituted derivatives (2°-phospha(III)amidines), the two possibilities are tautomeric. It is well known that amidines have restricted rotation about *both* the C=N double and the C–N single bonds due to allylic resonance.[49,52] This leads to four possible isomers designated

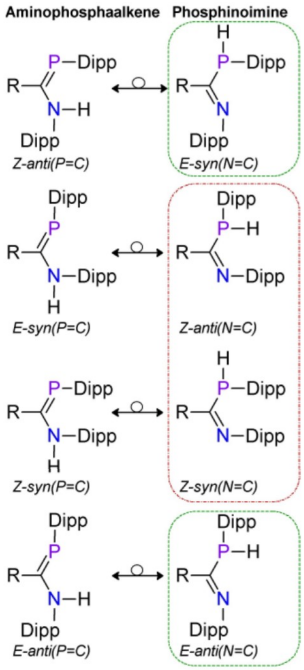

Scheme 3. Four *C*-amino-(σ^2,λ^3)-phosphaalkene isomers and potential *C*-(σ^3,λ^3)-phosphinoimine tautomers; rotation about P–C bonds collapses (N=C) to just *Z* (·–·–·) or *E* (– – –).

as *E-anti, E-syn, Z-anti* and *Z-syn*.[51,58] Our work and that of others have demonstrated that slow isomerization between several such isomers can be detected in solution on the NMR timescale in amidines with sufficiently bulky organic substituents on nitrogen and/or on the backbone C atom.[52,59] Calculations show even higher barriers to rotation about the C–N bond of *C*-aminophosphaalkenes than in their all-nitrogen counterparts. Hence, for *N,P*-disubstituted-*C*-aminophosphaalkenes, there are also four possible isomers, which we designate as *E-anti*(P=C), *E-syn*(P=C), *Z-anti*(P=C) and *Z-syn*(P=C), by a simple extension of the Häfeling & Kuske nomenclature.[51,58] For each of these isomers, there is in principle a *C*-phosphinoimine tautomer, which we designate with the (N=C) labels as drawn in Scheme 3 (where the tautomer of *Z-anti*(P=C) is *E-syn*(N=C) and that of *E-syn*(P=C) is *Z-anti*(N=C)). This potpourri of isomers and conformers has been investigated computationally by DFT calculations (see Figure 6). We say *in principle* because there is no evidence for the rigidity or otherwise of P–C_1 single bonds in the phosphinoimine isomers, although there are reasons to believe that the intrinsic barrier to rotation will be small in the absence of steric effects. If rapid rotation were possible, the *syn-anti* distinction of the (N=C) isomers would fall away but we are inclined to think that the bulk of the Dipp groups will induce some conformational specificity on these molecules.

Research Article
doi.org/10.1002/ejic.202300495

Synthesis

The synthetic route used to prepare **1a,b** involved thermal addition of either $DippPH_2$ or $DippPH(SiMe_3)$ to the isolated (by vacuum distillation) imidoyl chlorides in refluxing xylenes (Scheme 4).[60] Consumption of $DippPH_2$ was complete after about 5 days of heating (^{31}P NMR monitoring) during which the co-produced HCl was driven off. Unlike amidines,[49] **1** have much lower Brønsted basicity and protonated adducts were not observed under these conditions.[50] For **1b**, reaction progress was much slower; significant acceleration occurred by employing the monosilylated phosphane $DippP(H)Si(CH_3)_3$,[61] with complete reaction after refluxing in xylenes overnight. This reaction produced only **1b** – i.e. the leaving group is $ClSi(CH_3)_3$ and hydrogen is retained in the product. For the preparation of **4**, thermal reaction between $DippPH_2$ and *bis*(2,6-diisopropylphenyl)carbodiimide was not successful (as also observed with the all-N analogue)[53] so instead $DippPH^-Li^+$ was prepared *in situ* and used for the addition, followed by quenching the anionic product with water. This smoothly led to **4**, a rare compound of this type with two ionizable hydrogen atoms.

Molecular Structures in the Solid State

The identities of **1a,b** and **2** were established by EI mass spectrometry and the NMR and IR evidence also supported their molecular formulae. However, since the spectroscopic data is complex, we relied on single-crystal X-ray diffraction to establish the structures of these compounds in the solid state. Our discussion will therefore start out from this point. Deep yellow crystals of **1a,b**, obtained as blocks from slow cooling of hot solutions in methanol, are isostructural.[50,51] However, crystals of **1a** also grew from cold CD_3CN solution as a 1:1 solvate. This latter structure was determined at −100 °C and is more accurate than the RT structure reported earlier.[50] All three molecular structures are highly similar even regarding the relative orientations about the single bonds in the molecules and crystallize without any evidence of hydrogen bonding (not even to the acetonitrile of solvation) and without significant intermolecular contacts.

Both **1a** and **1b** crystallize with the *Z-anti*(P=C) amino-phosphaalkene isomer (Figure 1, Table 1). This result in itself implies that a 1,3-hydrogen shift has occurred because the hydrogen that is now located on N was introduced to the reaction by the phosphane;[62] the reaction was undertaken under careful protection from the atmosphere, so it is unlikely that water is involved in this transformation. The P1–C1 distances in **1a** and **1b** at 1.7225(7) and 1.7218(11) Å are indistinguishable at the 99% confidence level as are the N–C distances at 1.3596(8) vs. 1.3587(13) Å. These values are within the (very wide) range previously observed for amino-substituted phophaalkenes (1.70–1.76 Å P=C and 1.31–1.40 Å N–C[63]). In $MesP{=}C(Ph)NH_2$, the only other crystal structure reported of a *C*-amino-(σ^2,λ^3)-phosphaalkene containing an N–H bond (CSD refcode: ZEZSUS),[38] comparable distances are P=C 1.704(2) Å and N–C 1.357(3) Å. Residual electron density peaks near P

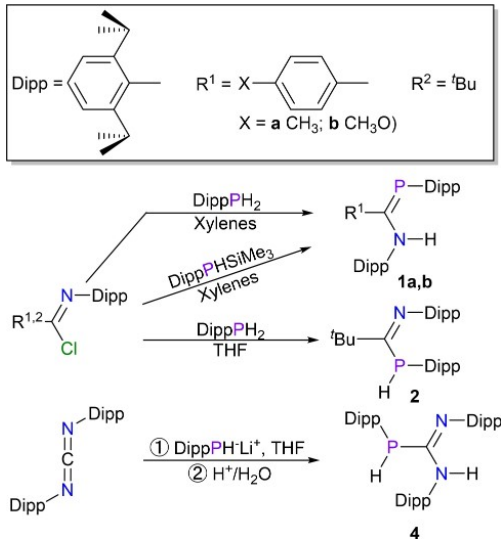

Scheme 4. Synthetic pathways employed.

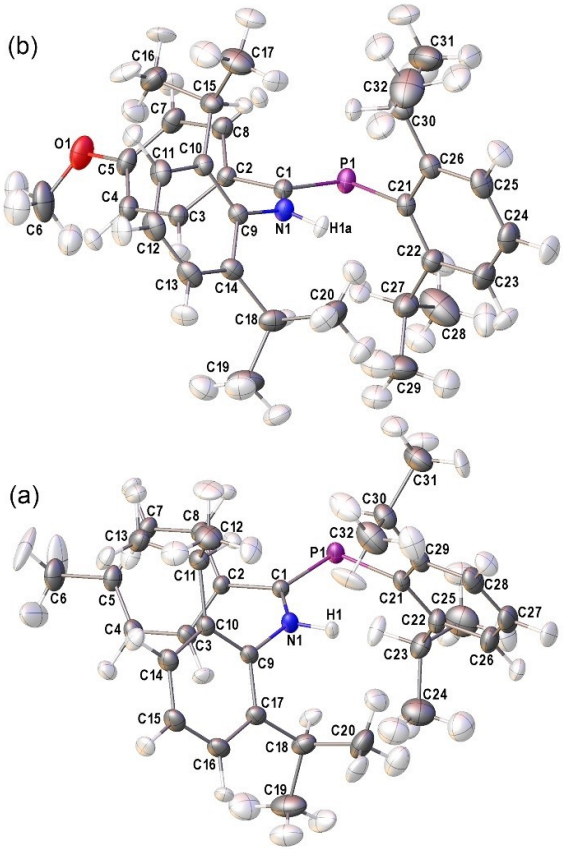

Figure 1. Plots of the molecular structures at −100 °C of (a) **1a** (the CD_3CN of crystallization and minor disorder ^{i}Pr component are omitted) and (b) **1b** as found in the crystals, with displacement ellipsoids drawn at 40%, from HAR/NoSpherA2[56] using aspherical form factors.

Research Article
doi.org/10.1002/ejic.202300495

Table 1. Key inter-atomic distances and angles for the phospha(III)amidine structures **1–4**.[a]

Dimension	1a	1b	2	3	4
P1-C1	1.7225(7)	1.7218(11)	1.8716(14)	1.868(3)	1.8725(8)
N1-C1	1.3596(8)	1.3587(13)	1.2729(15)	1.272(4)	1.2829(8)
Δ_{CN-CP}	0.363(1)	0.363(2)	0.599(2)	0.596(5)	0.590(1)
P1-H	–	–	1.377(16)	1.403(17)	1.359(9)
N1-H	1.001(9)	0.965(12)	–		0.987(10)
P1-C_{Ar}	1.8513(8)	1.8466(11)	1.8468(14)	1.829(3)	1.8427(8)
N1-C_{Ar}	1.4243(9)	1.4249(13)	1.4124(16)	1.411(4)	1.4119(9)
C1-C2(N2)	1.4825(8)	1.4782(14)	1.5279(18)	1.534(4)	1.3751(10)
Δ_{CN}	–	–	–	–	0.092(1)
N2-C_{Ar}	–	–	–	–	1.4308(10)
C1-P1-C_{Ar}	101.90(3)	103.00(5)	113.02(9)	102.48(14)	102.61(3)
C1-N1-C_{Ar}	129.58(6)	130.81(10)	123.26(16)	120.0(2)	122.21(7)
C1-N2-C_{Ar}	–	–	–	–	120.86(7)
P1-C1-N1	123.48(5)	123.10(8)	116.19(14)	123.0(2)	124.28(6)
N1-C1-C2(N2)	119.94(5)	121.29(9)	117.29(16)	118.6(3)	119.98(7)
P1-C1-C2(N2)	116.40(4)	115.42(7)	125.79(13)	118.3(2)	115.56(5)
$\Sigma\angle_{X-C1-Y}$	359.82(8)	359.81(14)	359.3(2)	359.9(4)	359.82(10)
C2(N2)-C1-P1-C_{Ar}	−168.97(5)	−175.89(8)	−25.0(2)	−129.0(2)	−27.71(6)
C2(N2)-C1-N1-C_{Ar}	−5.1(1)	−12.2(3)	−175.2(1)	−176.7(3)	−179.89(7)
N1-C1-N2-C_{Ar}	–	–	–	–	−17.5(1)

[a] HAR using NoSpherA2 for **1–4**.[56] For remaining inter-atomic data and other crystallographic parameters, consult the Supporting Information or deposited CIF data.

could be refined to partial H-occupancy, ostensibly from co-crystallized *E-syn*(N=C) *isomer* in both **1a,b** using standard refinement methods (the so-called Independent Atom Model)[56] but the occupancies (20% for **1a** and 10% for **1b**, Figure S7) exceed the evidence from solid-state NMR (see below). The minor isomer occupancies could not be substantiated by Hirshfeld Atom Refinement (HAR) using NoSpherA2[56] employing custom aspherical atomic scattering factors. A key advantage of HAR/NoSpherA2 for the structures refined in this paper is that it allows for near-neutron precision in placement of the hydrogen nuclei.[57] For an extended essay describing the crystallographic investigations, and an introduction to HAR/NoSpherA2, please see the Supporting Information. Infrared spectra obtained as KBr pellets show the expected ν(N–H) = 3351 and very weak ν(P–H) = 2374 cm^{-1} bands for **1a**. In solution these bands occur at (CH_2Cl_2): 3385, 3350 (N–H) & 2361 cm^{-1} (P–H); ($CHCl_3$): 3350 (N–H) & 2340 cm^{-1} (P–H); (heptane): 3354 (N–H) cm^{-1}. For **1b**, ν(N–H) = 3357 cm^{-1} as a solid in KBr; in solution these bands occur at ($CHCl_3$): 3350 (N–H) & 2389 cm^{-1} (P–H); (heptane): 3354 (N–H) cm^{-1} & 2401 cm^{-1} (P–H). Correlations of the computed IR spectra at the B3LYP–D3BJ/6-31G + (d,p) level of theory in a PCR continuum model for $CHCl_3$ solution of **1a** and **4** are provided in the Supporting Information.

The P-aryl to *ipso*-C bond, 1.8513(8) Å in **1a** agrees with the corresponding bond in DippP(H)Si^{t}Bu$(CH_3)_2$ (1.854(2) Å) at the 99% confidence level,[61] but the value for **1b**, 1.8466(11), is statistically short. The N-aryl bonds (1.4243(9) and 1.4249(13) Å) are within experimental errors of the values determined for the amino-aryl bond in the homologous bulky Dipp containing amidines (1.422(3) and 1.429(2) Å).[52] The C(21)-P(1)-C(1) angles (101.90(3) and 103.00(5)°) are noticeably smaller than the value found for the pure phosphaalkene MesP=CPh_2 (107.61(7)°; CSD refcode CENGEH01),[64] a known marker for aminophosphaalkene structures.[63] The P(1)-C(1)-C(2)-C(8) torsion angles show that the aryl groups are twisted from the P(1)-C(1)-N(1) plane, thereby minimizing steric interactions with the bulky Dipp groups. Additionally, the P-Dipp-^{i}Pr groups are twisted so as to minimize interactions with the phosphorus atoms, of which the latter are displaced by 0.153(1) and 0.308(1) Å from the mean aryl planes to the *opposite* side of the P=CR_2 substituent. This is typical of phosphorus environments containing *o*-^{i}Pr groups,[61] but is different than systems containing the Mes* (2,4,6-^{t}Bu$_3$C$_6$H$_2$) substituent where the phosphorus atom is displaced to the same side as the *ortho* 'R' substituents.[61]

Li et al. reported the synthesis and some spectroscopic data for **2** in 2009 but not the crystal structure of the phospha(III)amidine itself.[41] In view of the high interest in comparing **2** directly with **1** (which have identical Dipp groups on both N and P and thus differ only in the ^{t}Bu versus aryl substituents on the backbone carbon of the phospha(III)amidine), we have synthesized this compound by the reported method and determined its structure by XRD at low temperature (Figure 2a, Table 1). Unlike **1**, **2** crystallizes

Research Article
doi.org/10.1002/ejic.202300495

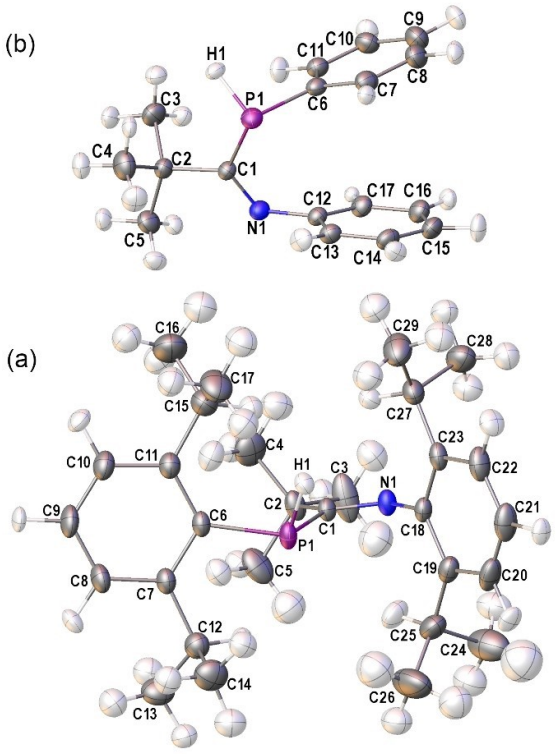

Figure 2. Displacement ellipsoids plots (40% probability) of (a) **2** and (b) **3** as found in their crystal lattices at −100 °C. HAR undertaken with NoSpherA2 in Olex2. The minor components of the disorder in the structure of **2** are omitted (see Supporting Information for details).

unambiguously as the *Z-anti*(N=C) phosphinoimine isomer with a distinctly pyramidal phosphorus atom bearing the hydrogen atom (Figure 2a). Difference Fourier syntheses do not show any electron density that might correspond to an H atom on N from a C=P isomer co-crystallized in the lattice; also the crystals are colourless whereas aminophosphaalkenes of this genre are typically bright yellow. However, there is positional disorder for the P atom (see Supporting Information for a description of the satisfactory disorder model). Consistently, the P–C distance at 1.8716(14) Å is longer than the average value of 1.722(1) Å in **1** by 8.7% and the N=C value of 1.2729(15) is 6.3% shorter than the average 1.3592(15) Å in **1**; bond length differences of this magnitude represent significant differences in bonding.

The conformation adopted by **2** is quite similar to that of **1** if the P and N atoms are swapped (both are formally *Z-anti*), but the EH groups differ since the phosphorus is as expected much more pyramidal than is the N atom in any of these structures. One consequence of the pyramidal phosphorus is considerable twisting about the P–C single bond, whereas **1a,b** are essentially co-planar. Comparable structures are hard to find, but a diphospha(III)amidine, also with ^{t}Bu backbone and P-Mes substituents displays such a torsion as 133.80(9)° (CSD refcode: BILBAA),[23] whereas the all-N analogues of **1a** and **1b** display 175.4(4)° and 173.9(1)°, respectively (refcodes: GOBNIU, GOBMOZ).[52] While rotation about the C1–P1 bond may have a low intrinsic barrier, it seems quite likely that full rotation would be impeded by collisions between the ^{i}Pr methyl groups of the Dipp substituent and the ^{t}Bu group on the backbone. To get a preliminary insight into this value, a simple relaxed-scan DFT calculation at the B3LYP/6-31G(2d,2p) level of theory in the gas phase was undertaken for rotation about the P1–C1 bond in **2** using coarse 20° steps (the calculation is very time consuming). A computed barrier of only about 33 kJ/mol is required to rotate from the global minimum *Zanti*(N=C) to a second minimum only 9 kJ/mol higher in energy that is very close to fully optimized *Zsyn*(N=C); for details see Figure S25 in the Supporting Information.

Many years ago, Issleib *et al.* reported the synthesis of some trimethylsilyl derivatives of phospha(III)amidines derived from phenylphosphane, $PhPH_2$.[21b] In our hands, these materials are extremely unpleasant to handle, forming intractable tars and oils and possessing a highly unpleasant odour. The initial report also claimed that exchange of $Si(CH_3)_3$ with H by methanolysis afforded an N=C isomer, based on solution NMR evidence. We obtained suitable crystals of ^{t}BuC(NPh)(PHPh) as colourless prisms from slow hydrolysis of the silyl compounds and a crystal structure of surprising quality was determined and successfully refined using HAR/NoSpherA2 with accurate placement of H-nuclei (Figure 2b, Table 1).[65] As shown in Figure 2b, the conformation adopted by **3** in the crystal lattice is extremely close to the DFT-optimized geometry for **2** in the *Z-syn*(N=C) isomer/conformer (Figure S26). The value of the N1-C1-P1-C6 torsion angle is 55.3(3)°, so that the NCP plane effectively bisects the H1-P1-C6 angle. This conformation will turn out to be of great importance in the bonding analysis by DFT. In organic amidine chemistry in general, this conformer (*Z-syn*) is adopted most commonly when the backbone substituent is ^{t}Bu.[49] In phosphorus derivatives, it is known for a very unusual structure of a diphospha(III)amidine where the H on P is replaced by Cl/Br (CSD refcode: HUXPIZ),[66] for which the P=C-P1-C_{ispo} torsion angle is a very similar 62.6(1)°. Consideration of the structure of **3** sheds immediate light on its conformational preference: this geometry affords close to ideal phenyl ring π-stacking with ring-centroid to nearest ring C distances as low as 3.40 Å.[67]

In this structure, the P–C distance at 1.868(3) Å is longer than the average value of 1.7222(13) Å in **1** by 8.5% and the N=C value of 1.272(4) is 6.7% shorter than the average 1.3592(15) Å in **1**. Other metric values are also quite similar to those found in **2** with the major exception of the C1-P1-C_{Ar} angle which at 102.49(17)° is 8.3% smaller than the corresponding value in **2**, presumably due to the much smaller steric demand of the Ph versus the Dipp substituents. The crystal structure of **3** shows no evidence of positional disorder of the H atoms on P.

A good quality low temperature crystal structure of **4** has been determined (Figure 3, Table 1), apparently the first to be reported of an *N,N′,P*-trisubstituted monophospha(III)guanidine, which shows unambiguously that the geometry is *N*H,*P*H and hence an N=C rather than a P=C isomer. This is fully consistent with the spectroscopic data (see below) and the colorless nature of the compound, whereas Dipp-substituted amino-

Research Article
doi.org/10.1002/ejic.202300495

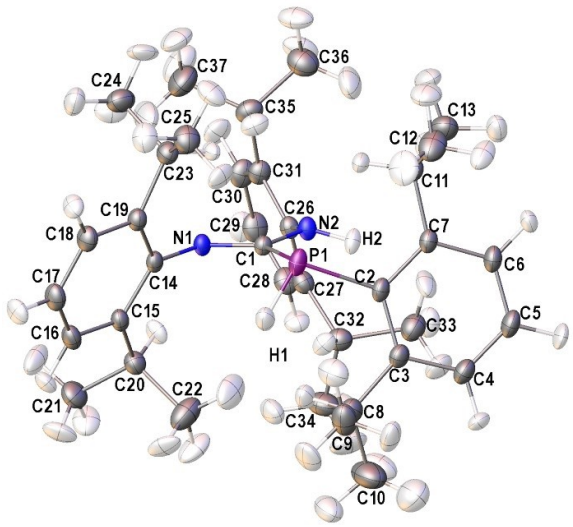

Figure 3. Displacement ellipsoids plot (40% probability) of the molecular structure of **4** as found in the crystal at −100 °C. HAR undertaken with NoSpherA2 in Olex2 with accurate H-atom placement.

phosphaalkenes are consistently bright yellow. The conformation adopted by **4** is highly reminiscent of that determined for **2** (Figure 2). The phosphorus atom is quite pyramidal, the substituents are in similar orientation and thus this phospha(III)guanidine can be described as a *Z-anti*(N=C) phosphinoimine bearing a DippNH substituent at C1.[55]

In this structure, the P–C distance at 1.8725(8) Å is statistically indistinguishable from this bond type in **2** at the 99% confidence level and longer than the average value of 1.722(1) Å in **1** by 8.7% and the N=C value of 1.2829(8) Å is 5.6% shorter than the average 1.3592(15) Å in **1**. Other metric values are also quite similar to those found in **2** and **3**; interestingly the C1-P1-C_{Ar} angle is much closer to that in **1** than the corresponding value in **2**, suggesting that the steric pressure extended by a DippNH substituent is considerably less than ^{t}Bu. The N1-C1-P1-C2 torsion angles of **2** and **3** are very similar. Overall, the structure of **4** demonstrates less steric congestion than in **2** with atoms largely co-planar with the attached aromatic rings, and it shows no evidence of positional disorder of P or H atoms. However, as for all N=C phospha(III)amidine derivatives in this study, the pyramidal P atom is rotated out of the N=C-N plane to a considerable extent (see bonding section).

Previously there have been reports of both N=C and P=C monophospha(III)guanidines. For example, the group of Martyn Coles have conducted extensive studies of conformations and isomerism in $R_2PC(=NR')(NHR')$ as well as the coordination of the deprotonated amidinate unit.[33,34] In these molecules, double substitution at phosphorus prevents tautomerism *between* N and P. Other workers have contributed to the chemistry of $RP{=}C(NR'_2)_2$, fully substituted diaminophosphaalkenes, where the possibility of tautomerism is also shut down.[32,63] Fascinatingly, both N=C and P=C isomers of monophospha(III)guanidines have recently been produced by addition of amines to phosphinidene isonitrile adducts, wherein the reactant and products are all stabilized by coordination to $W(CO)_5$.[68]

The structure of **4** can also be described as an amidine bearing DippPH as a backbone substituent; from this perspective the structure may be compared with several *N,N'-bis*(Dipp)amidines that have been structurally characterized previously.[52,53,59] The difference in lengths of the C=N and C–N bonds, $\Delta_{CN} = 0.093$ Å, in **4** is one of the largest that has been reported to date for any amidine, but similar to those reported by Coles et al.[43] The amidine conformation is the common *E-syn* isomer; however the conformation about the C1–P1 bond (N2-C1-P1-C_{Ar} torsion angle) is in between the α and β conformational designations developed by Coles et al. but very similar to that found in the crystal structures of $Ph_2PC(=NR)(NHR)$ {R = ^{i}Pr, Cy} (torsion angles of 0.0 and 10.6°, respectively; CSD refcodes: OHIQUR, OHIRAY).[24] However, the closest analogue structure to **4** in the literature is $Ph_2PC(=NDipp)NHDipp$ (refcode: DOQFAR).[69] This structure, unlike the closely-related $CyPh_2PC(=NDipp)NHDipp$ (refcode: DOQDUJ), has the same *E-syn*(N=C) geometry *at the amidine moiety* as **4**. The structure bears a striking resemblance to that of **4** with the "second" Ph group having almost the same orientation as the H atom on P in our structure (torsion angles of 83.0(1)° and 53.2(4)°). However, the bond distances reported for this compound diverge significantly. Thus, the P–C distance at 1.8798(18) Å is longer than the value 1.8725(8) Å in **4**, a difference that exceeds the 99% confidence level for the bonds to be the same. More dramatic is the $\Delta_{CN} = 0.035$ Å in their structure, whereas this value for $CyPh_2PC(=NDipp)NHDipp$ is 0.0841 Å, very much closer to that in **4**. Perhaps significantly, the Ph_2P species is reported by the authors to exist as an *E-syn*/*Z-anti* mixture in solution while that Cy_2P species is solely *Z-anti*; it could therefore be that the reported structure of $Ph_2PC(=NDipp)NHDipp$ is actually a co-crystallization of tautomers as occurs in the all-nitrogen analogue of **1a**, because the major ramification of such tautomerism is exchange of the C–N single and double bonds.[52]

Reactivity

As previously reported, deprotonation of **1a** with *n*BuLi in THF afforded the $Li(THF)_3^+$ complex, while potassium bistrimethylsilylamide, in the same solvent, afforded a more complex, polymeric, structure wherein one potassium ion is coordinated to nitrogen and a second to phosphorus atoms.[50] Coordination chemistry of **1** to Cr, Mo and W $M(CO)_5$ moieties in κP mode has also been demonstrated.[51] Li et al. have reported similar adducts of **2** (Li^+ salt and Tl^+ adducts).[41] Coordination of deprotonated phospha(III)amidinates has been reported by Lammerstma et al.[15,60] and Mankad et al.[62] In this work, we obtained evidence for the reactivity of the monophospha(III)guanidine **4** with oxygen, corroborated by crystallography. We also have some limited, but fascinating, evidence for phosphinidene transfer reactivity from **1** upon longer storage. There have been intensive efforts over decades to prove the existence of phosphinidenes,[70] and cyclic

Research Article
doi.org/10.1002/ejic.202300495

polyphosphanes have been postulated as *sources* for them, but to our knowledge there is no previous record of the reverse reaction having occurred.[71] Since, however, there is only limited evidence available, this additional reactivity has been located in the Supporting Information. A detailed investigation of the electrochemistry of **1 a**, complete with a mechanistic and computational analysis is also reported in the Supporting Information. Here too, the limited scope and lack of comparison to the other species do not warrant inclusion in the main article.

Solution and Solid-State NMR Characterization

A thorough NMR study of **1 a,b** was undertaken using a multinuclear approach. Highly purified crystalline samples, when dissolved in purified NMR solvents in sealed sample tubes under vacuum, repeatedly show the presence of up to four isomers in solution. We start this discussion with the ^{31}P NMR spectrum of **1 a** in $CDCl_3$ solution (Figure 4) in which four sets of signals are visible. Careful integration indicates that the largest signal is a singlet at +53.6 (87%), followed by a narrow doublet at +79.5 ppm (J_{PH} = 10 Hz, 10%), a wide doublet at −80.3 (J_{PH} = 243 Hz, 3%) and another wide doublet at −66.4 (J_{PH} = 243 Hz, <1%) ppm. In the ^{1}H spectrum, the three major species are readily identified from the J_{PH} values and by integration as 6.23 (J_{PH} = 6.23 Hz, 87%, NH), 5.91 (J_{PH} = 11 Hz, 10%, NH) and 4.92 ppm (J_{PH} = 242 Hz, 3%, PH). The fourth species could not confidently be detected in ^{1}H NMR spectra, due to low intensity and the high likelihood of signal overlap. Very similar spectra are obtained for **1 b**, so that the behaviour is parallel to that of **1 a** (see the Supporting Information).

Assigning such a plethora of signals poses a significant challenge. In this case, we are greatly helped by solid-state NMR. Thus, the pure yellow and highly uniform crystalline samples of **1 a** which are known from crystallography to be the *Z-anti*(P=C) isomer (see above) were subjected to a solid-state ^{31}P NMR study. Experiments were run with direct polarization, cross-polarization (CP) and CP with ^{1}H decoupling. The later gives the best resolution and is shown in Figure 5. The observed

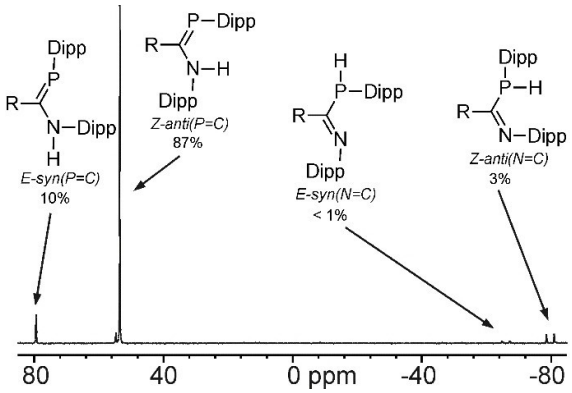

Figure 4. ^{31}P NMR spectrum of **1 a** in $CDCl_3$ (purified material in dry solvent, vacuum sealed, obtained without proton decoupling).

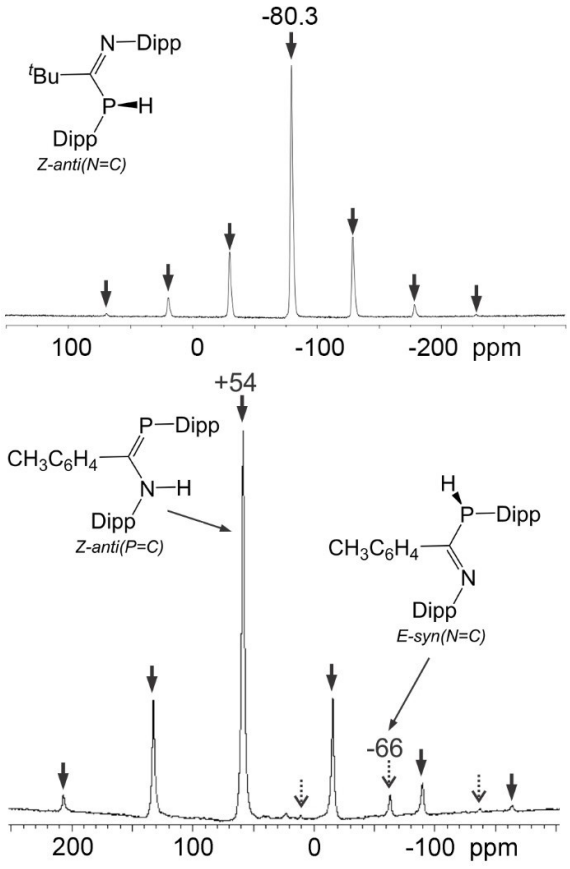

Figure 5. Proton decoupled ^{31}P CP-MAS solid-state NMR spectra of (lower) **1 a** spun at 15 kHz and (upper) **2** spun at 10 kHz. The solid arrows designate the major signals and their spinning side-bands; the dashed arrows designate the minor signal component in **1 a** with its side-bands.

spinning side-band patterns show a quite symmetrical shielding tensor with the expected 15 kHz spacing (~54 ppm between lines). But there is a second signal, also with 15 kHz side-bands, at ~−66 ppm. It seems a reasonable assumption that this signal emanates from some co-crystallized *E-syn*(N=C), i.e. that tautomer in which the orientations of the substituents are very similar (whether actual co-crystallization is present, or whether these are mixtures of pure crystals of the two compounds with identical solubility characteristics is immaterial to this argument). This assumption allows the solution species at +53.6 ppm in $CDCl_3$ to be identified as the *Z-anti*(P=C) and that at −66.4 ppm as the *E-syn*(N=C) isomer.

It remains to assign the other two species. The larger 10 Hz $^1J_{PH}$ coupling of the +79.5 ppm signal is characteristic of *E* configuration and along with the positive shift makes an excellent fit to *E-syn*(P=C). This is the same criterion as used to assign the solution isomers of R_2P–C(=NDipp)NHDipp.[69] The relative chemical shifts of the P=^{13}C signals by comparison with *E,Z* phosphaalkenes substantiates this as an *E* isomer.[72] The only reasonable alternative, i.e. *E-anti*(P=C) is a much poorer fit to the detailed ^{1}H, ^{13}C and two-dimensional NMR evidence. Full details are provided in the Supporting Informa-

Research Article
doi.org/10.1002/ejic.202300495

tion. Furthermore, in general *E-anti* geometries for amidines are rare in solution except in the case of formamidines; for *N,N'*-formamidines, this geometry is stabilized by face-to-face (amine to imine) hydrogen bonding, but we would expect such H-bonded dimers to be much weaker in the case of phospha(III)amidines. The final assignment, that the −80.3 ppm signal is its tautomer, *Z-anti*(N=C), seems very reasonable as neither *E-anti* nor *Z-syn* are likely candidates, the latter on steric grounds. Here too there is evidence from the remaining NMR data. A thorough examination by NMR of **1** was undertaken, always in sealed sample tubes filled under N_2 protection, in deuterated NMR solvents benzene, toluene, acetone and methanol. The more polar the solvent, the larger the proportion of the *E-syn*(P=C) relative to the *Z-anti*(P=C) which become equal in CD_3OD. The proportion of N=C tautomers remains small in all solutions, but is always detectable, especially via ^{31}P NMR. A ^{1}H-NMR EXSY experiment in $CDCl_3$ was also conducted on **1a** (see below). Interestingly, in $(CD_3)_2C=O$, the P–H signals of the two (N=C) isomers convert to triplets from $^{1}H/^{2}D$ exchange (as monitored by ^{1}H-coupled ^{31}P NMR spectroscopy). Since phosphines do not easily exchange with deuterium in R_2PH but such exchange is facile in amines, this observation supports the notion of a solution equilibrium between these P=C and N=C isomers. Notably, solutions of **2** are stable for long periods of time in $(CD_3)_2C=O$ with no noticeable deuterium incorporation.

NMR characterization of 2. The ^{31}P NMR spectrum of **2** in $CDCl_3$ solution is a sharp doublet with $\delta = -84.73$ and $^{1}J_{P,H} = 251$ Hz, fully consistent with the N=C isomeric geometry. Solid-state MAS ^{31}P NMR spectra (Figure 5) taken from the same crystals used for the SC-XRD display a highly symmetric set of spinning side bands from the 10 kHz spinning, indicative of a symmetric shielding tensor. The chemical shift at −80.3 ppm is in excellent agreement with the solution value and gives high confidence that the molecule retains the *Z-anti*(N=C) conformation in solution. The ^{1}H NMR spectra are also informative (Figures S19,S20). The P–H signal is readily identified at $\delta = +4.74$ and $^{1}J_{P,H} = 250$ Hz. The ^{i}Pr-CH_3 groups form 6 doublets, integrating to 24 hydrogens. The ^{i}Pr-CH protons form three sets of peaks, one broad peak corresponding to the phosphino Dipp group, and two sets of septets corresponding to the amino Dipp group. The aromatic signals for CH_{meta} forms four doublets and for CH_{para} forms two triplets for the amino and phosphino Dipp groups. Most noticeable in the ^{1}H NMR spectrum is the difference between signals from the DippN and DippP rings. For example, in the ^{i}Pr-CH signals, there is a single featureless broad peak for DippP (implying equivalence for both substituents, which appear as a coalesced signal due to rapid exchange of the two isopropyl groups). The two CH groups can exchange by rotation about the $C_{backbone}$-P bond (see above under the SC-XRD for computational investigations of such rotation). But there are two different, resolved, septets for the DippN, implying that the two substituents are inequivalent. Moreover, the upfield signal is somewhat line broadened compared to the more downfield multiplet. Importantly, there was no evidence for the presence of multiple isomers (neither *E/Z* isomers nor tautomers) in any NMR spectra undertaken on **2**, in strong contrast to what is observed for **1**.

Solution NMR characterization of 4. In solution as studied by NMR, **4** also shows little evidence of isomerism, irrespective of the solvent employed. The ^{31}P spectrum consists of the expected doublet (δ −94.8 ppm, $^{1}J_{PH} = 237$ Hz) for coupling to the directly bonded H atom. This doublet also occurs in the ^{1}H NMR in $CDCl_3$ solution (δ 4.87 ppm, $^{1}J_{PH} = 237$ Hz). The NH signal is a singlet at $\delta = 5.35$. This is entirely consistent with the solution structure retaining the *E-syn*(N=C) geometry *at the amidine* whereby the NH proton is *syn* to the P atom. This is in full agreement with $Ph_2PC(=NDipp)NHDipp$ (NH singlet) and $CyPh_2PC(=NDipp)NHDipp$ (NH doublet with $^{3}J_{PH} = 18.2$ Hz, since the latter is assigned the *Z-anti*(N=C) amidine geometry.[69] However, unlike the reports for these important comparison compounds, the full ^{1}H NMR of **4** is complicated by dynamic effects that cause two of the septets to be coalesced and four of the six ^{i}Pr methyl doublets also to be coalesced (see Supporting Information). By analogy to $DippN=C\{NHDipp\}_2$, we believe this behaviour in **4** is caused by rotations of one of the Dipp groups attached to the central carbon atom and not by isomerisation (note that the NH and PH signals remain sharp and are apparently not involved in the exchange.)[53] At the current time we have not been able to study these dynamic effects in **4** in greater detail, but the lack of effect on the NH resonance at RT is consistent with slowed rotation about the P–C single bond; the two longer P–C ($P–C_{Dipp}$ and $P–C_{guan}$) bonds should also lead to lower barriers for rotation compared with the N–C bonds. Slow rotation of the "backbone" substituent was also attributed to the $Mo(CO)_3$ "piano-stool" complex of $DippN=C\{NHDipp\}_2$, further supporting our hypothesis.[53,73]

Computed Structural Models by DFT Calculations

We have performed B3LYP/6-31G(d) calculations on all eight possible isomers and tautomers of **1a** and of **2**. The calculated structures are displayed in Figure 6 for **1a** (and Figure S26 for **2**). The calculated relative energies of these systems are presented in Table 2. As the molecules are very large, only the small double-ζ wavefunctions could be employed, but there is gratifying agreement between these simple hybrid DFT calculations and the experimental results. We recognize that, with so many significant internal steric interactions, and with such small energy differences, that our optimized (frequency-verified) geometries probably have not explored the full energy surfaces. Also, in view of the large hydrocarbon substituents, the role of dispersion in the steric interactions could not be ignored. Hence, all the calculations have been repeated using Grimme's D3 empirical dispersion correction (with Becke-Johnson damping).[74,75]

There are some changes in energy predictions with and without the dispersion corrections. Gratifyingly, both methods predict the lowest-energy species as *Z-anti*(P=C), the structure adopted by **1a,b** in the crystals that we examined and convincingly the major species in solution by NMR. In the case

Research Article
doi.org/10.1002/ejic.202300495

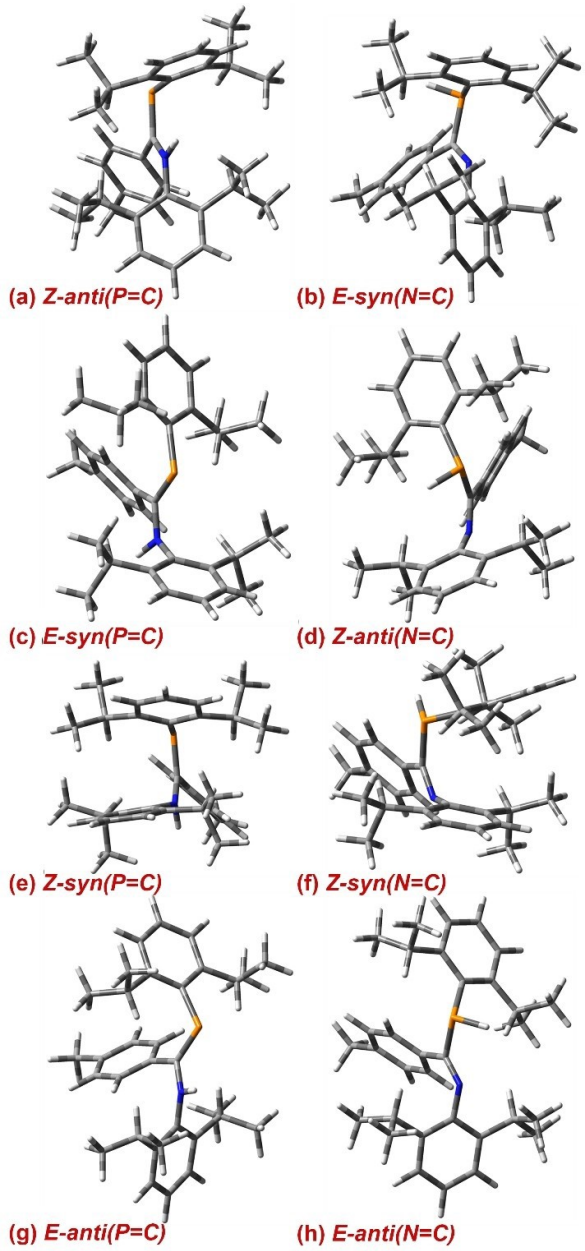

Figure 6. B3LYP/6-31G(2d,2p) calculated geometries of aminophosphaalkene isomers of **1 a** (left) arranged beside their phosphinoimine tautomers (right).

of **2**, the lowest and next-higher energies switch between *Z-anti*(N=C) for DFT and *Z-syn*(N=C) for DFT-D3BJ, with a difference of 8–9 kJ/mol between them. This corresponds directly to the computed scan for rotation about the P–$C_{backbone}$ single bond mentioned previously (Fig. S25), and the preference for *Z-syn*(N=C) with dispersion correction reflects the strong attraction between the DippP aromatic ring and ^{i}Pr groups on the DippN ring. These computational results are thus fully consistent with the ^{1}H NMR evidence for fluxionality about this P–C bond in solution at ambient temperatures. Both of these optimized structures display the Dipp–P–H moiety rotated significantly out of the C=N-C plane, similar to the computed *Esyn*(N=C) conformer of **1 a**.

The next-higher isomer for **1 a** is *E-syn*(P=C), at 8 kJ/mol only slightly higher in energy, consistent with this being the second-highest abundant solution species by NMR in most solvents. Also gratifying is that the next four higher-energy calculated species are all *N=C* isomers, with *Esyn*(N=C) and *Z-anti*(N=C) effectively equal in energy by both approaches, which again fits well with the geometries assigned via the NMR investigation. The only anomaly is that dispersion correction assigns *Z-syn*(N=C) as the #2 species for **1 a**, again highlighting the likely dispersive overcorrection in this sterically congested tautomer.[67] Importantly, the combined effects of steric interactions between the bulky substituents and the not-insubstantial mixing of the core orbitals of the allylic fragment with the carbon atoms of the aromatic substituents washes out the large preference for the P=C isomer demonstrated for the all-hydrogen parent compounds (see below). Of particular interest to this work are the quite low computed energies of *Z-syn*(N=C) for both **1 a** and **2**. A consideration of Figure 6(f) shows that this is due to the significant twist at the P–C bond which allows the two superimposed Dipp groups to minimize ^{i}Pr to ^{i}Pr steric clashes; this is *not* possible for *Z-syn*(P=C), Figure 6(e), because of the substantial barrier to twisting about the *pseudo*-N=C bond of the aminophosphaalkene. What is more difficult to understand from the computational study is why tautomerism is not observed to produce (P=C) isomers in solution for **2**, since the predicted energy differences are small (the lowest P=C form is computed to be only 10 or 17 kJ/mol higher than the lowest N=C form, without and with dispersion correction, respectively).

*Electronic structures of isomers of **1 a**.* We restrict our discussion to a comparison between the frontier molecular orbitals (FMOs) of *Z-anti*(P=C) and *Z-anti*(N=C); other isomers compare similarly (Figure 7). The five highest lying filled orbitals in the (P=C) isomer all lie substantially higher in energy than those in the (N=C) isomer. The LUMO has N–C=P π(3) character albeit with substantial delocalization into the tolyl backbone substituent despite a tilt of this ring of some 45° out of plane. The HOMO, at −5.12 eV, has dominant π(2) character and corresponds principally to the P=C π-bond. The next lower orbital is the *n*(P) lone pair orbital which is considerably delocalized into the aromatic ring of the Dipp group attached to phosphorus. The next five lower-lying MOs are all π orbitals associated with the three aryl rings in **1 a**. The HOMO-10 is the most clearly identifiable N–C=P π(1) MO, and is definitely localized onto the N–C component of this strongly allylic π-system. In the (N=C) isomer, the LUMO has distinct π′(2)* character, while π′(1) is the very stable HOMO-8 although this character is spread over several FMOs. The main orbital with P lone pair character is HOMO-4. The HOMO, largely of Dipp ring π(3) character, is found almost 0.6 eV *lower* in energy, with the counterintuitive result that a molecule that is some 19 kJ/mol *less* stable has a significantly lower-lying HOMO and a larger HOMO-LUMO gap.

Figure 8 presents the FMOs of the 100% occupied *Z-anti*(N=C) isomer of **2**, in contrast to **1 a** where this tautomer is a higher energy form that is only 3% abundant by NMR

Research Article
doi.org/10.1002/ejic.202300495

Table 2. Relative energies (kJ/mol) of the phospha(III)amidine conformers and tautomers from DFT.

Geometry	Tolyl[a] B3LYP	Tolyl[b] B3LYP-D3BJ	Tolyl Obsv. % in ^{13}P NMR	^{t}Bu[a] B3LYP	^{t}Bu[b] B3LYP-D3BJ	^{t}Bu Obsv. % in NMR
Z-anti(P=C)	0	0	XRD, 87	+9.8	+16.8	n/o
E-syn(N=C)	+15.6	+18.2	<1	+22.7	+29.3	n/o
E-syn(P=C)	+8.4	+12.5	10	+14.2	+25.0	n/o
Z-anti(N=C)	+15.6	+18.6	~3	0	+8.5	XRD, 100
Z-syn(P=C)	+39.5	+30.9	n/o[c]	+29.1	+20.3	n/o[c]
Z-syn(N=C)	+18.5	+8.8	n/o[c]	+9.3	0	[c]Disp.?[d]
E-anti(P=C)	+17.6	+22.0	n/o[c]	+42.5	+42.5	n/o[c]
E-anti(N=C)	+22.5	+38.0	n/o[c]	+22.5	+22.5.0	n/o[c]

[a] Computed at the RB3LYP/6-31G(2d,2p) level of theory. [b] Computed at the RB3LYP–D3(BJ)/6-31G+(d,p) level of theory (including dispersion correction). All isomers and conformers are local minima from frequency calculations. [c] Conformer, may not be distinguishable in solution. [d] A conformation that is likely to be favoured by dispersion, as observed e.g. in the SC-XRD of **3**.

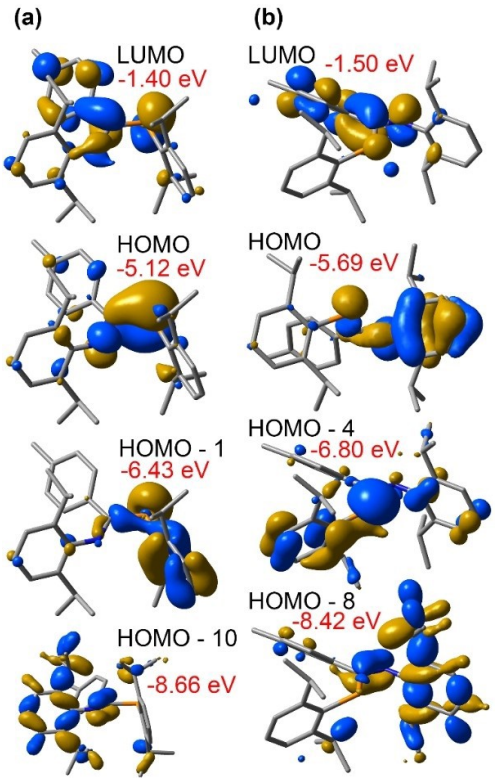

Figure 7. Kohn-Sham orbital isosurfaces from DFT-dispersion corrected calculations on **1a** in (a) the energetically lowest energy *Z*-anti(P=C), and (b) **1a** the higher-energy *Z*-anti(N=C), geometry showing the Frontier Molecular Orbitals.

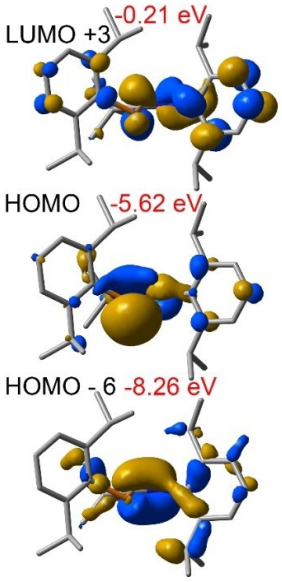

Figure 8. Kohn-Sham orbital isosurfaces from DFT calculations on **2** in the lowest-energy *Z*-anti(N=C) geometry showing the FMOs.

integration (Figure 4). There are significant differences between the orbital manifolds of the *Z-anti*(N=C) isomers of **1a** and **2**. The FMO with distinct N=C $\pi'(2)^*$ character in **2** computes as LUMO+3 (the intervening virtual orbitals have predominantly ring π^* character) but also involves some *n*(P)* character. The HOMO (also fairly stabilized at −5.62 eV) has predominant *n*(P) character and is more energetic than the *n*(P) HOMO-1 of *Z-anti*(P=C) in **1a**, which is a known donor towards zerovalent Cr, Mo and W.[51] The corresponding HOMO-6 N=C $\pi'(1)$ orbital is, however, greatly stabilized and has a significant *n*(P) contribution. Very likely, the *n*(P) overlap is a factor in the significant out of plane tilting of the DippPH moiety in all the computed and crystallographically characterized N=C isomers encountered in this study.

Computed structural models of monophospha(III)guanidine ***4***. Full B3LYP-D3BJ/6-31+G(d,p) dispersion-corrected optimizations for the guanidines have been restricted to six representative geometries. First of all, the *Z-anti*(N=C) isomer as found in the crystal lattice of **4** was optimized starting from the XRD molecular structure. This molecule optimizes to a very similar geometry, and specifically the N2-C1-P1-C_{Ar} torsion angle (see Figure 3) computes to −31.6° compared to experimental −27.71(6)°. We are hopeful that nature has chosen the optimal conformation for this sterically crowded molecule. The same

Research Article
doi.org/10.1002/ejic.202300495

conformation, save that the torsion reduces to −5.8° is maintained in the *Z-anti*(P=C) isomer, which is remarkably computed to be only 5.8 kJ/mol higher in relative energy. The remaining selected structures, pre-optimized from the above two using the PM6 semi-empirical method, optimized to: *Z-syn*(N=C) at +7.4; *E-anti*(N=C) at +14.0; *E-syn*(N=C) at +16.7 and *Z-syn*(P=C) at +37.3 kJ/mol. Structure definitions are taken for the N=C isomers by treating the DippPH- group as a substituent at the amidine. The geometry selected for naming the P=C isomer is *Z-anti* for the first DippNH group and *E-syn* for the second, the only conformation that results in the same C_3 "paddlewheel" motif as found in SC-XRD of **4**, which obviously minimizes steric congestion amongst the three bulky Dipp groups. Structure diagrams are available in Figure S27 of the Supporting Information. Evidently, the "paddlewheel" N=C structure that crystallizes and dissolves (NMR evidence) does seem to be the lowest energy choice. It is remarkable how small the energy difference between the same nominal conformation in the two isomeric N=C and P=C forms is; we stress again that no evidence was found by NMR, in several solvents, more and less polar, than $CDCl_3$, for the aminophosphaalkene isomer, nor in the solution-phase FTIR spectra.

Key FMOs for the ground state structure of **4** are presented, with their energies, in Figure 9. The LUMO+2 virtual orbital corresponds to the allylic amidine π(3)* orbital. The HOMO, most interestingly, has *n*(N) character, albeit delocalized into the DippN aromatic π(3) component, which evidently raises the energy of this donor site. HOMO-1 and HOMO-2 together correspond to the amidine π(2), effectively non-bonding FMOs, concentrated on the N atoms, while each is delocalized into an occupied Dipp aromatic MO. It is not until HOMO-4 that an FMO is found with significant *n*(P) character, at the low energy of −6.67 eV. We should therefore not expect **4** to be a good phosphorus donor in metal coordination. HOMO-7 is a most significant FMO, for it shows heavy *n*(P) delocalization into the allylic amidine π(1) FMO, a characteristic that may be a driving force in the out of plane rotation of the DippPH moiety (as in the FMOs of **2**).

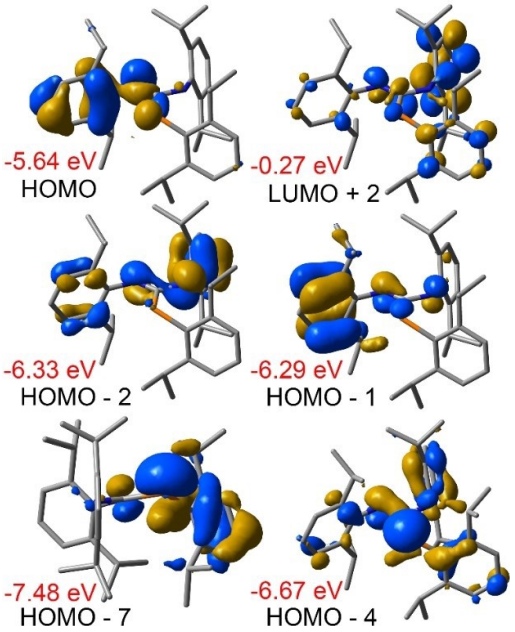

Figure 9. Kohn-Sham orbital isosurfaces from DFT calculations on **4** in the energetically lowest energy *Z*-anti(N=C) geometry showing the Frontier Molecular Orbitals.

Further Considerations of Electronic Structure: The Parent Compounds

In order to gain deeper insight into the very subtle isomeric preferences of the phospha(III)amidines investigated in this report, we have also modelled possible isomers, tautomers and rotamers of the parent structures using larger basis sets than were feasible for the full compounds. Thus, we have studied the isomeric and tautomeric preferences for the parent heteroallylic species with H in place of all the organic groups. Here the conformational choices simplify to four possibilities: *E*(P=C), *Z*(P=C), *E*(N=C) and *Z*(N=C). The B3LYP/6-311G++(3df,2pd) hybrid DFT method was employed and results are shown in Table 3 and Figure 10. The relative energies of the four refined geometries are: *Z*(P=C) = 0, *E*(P=C) = +2.5, *Z*(N=C) = +22.1, *E*(N=C) = +22.5 kJ/mol. These calculations show that the experimentally observed major isomer for **1** that is *C*-amino-(σ^2,λ^3)-phosphaalkene corresponds to the lowest energy gas-phase isomer of the parent molecule. However, compared to the fully C substituted analogs **1** and **2**, the energy differences between this and the *C*-(σ^3,λ^3)-phosphinoimine alternative is *much larger* for the all-H case. No previous computational study appears to have directly compared P=C and N=C isomers of the parent phospha(III)amidines.

Others have, however, investigated *E*/*Z* isomerism in *C*-amino-(σ^2,λ^3)-phosphaalkenes. Our results may be compared to those of Prasad et al. who obtain *E*(P=C) = +2.9 kJ/mol at the MP2/6-31G(d) level of theory compared to *Z*(P=C).[76] The bond distances of our calculations agree better with the experimental average in **1** of 1.7222(13) and 1.3592(15) Å for distances 1 and 2 than obtained from the MP2 calculations. Wiberg found *E*(P=C) = +3.0 kJ/mol at the MP2(fc)/6-31+G(d) level.[77] Schoeller has apparently calculated the *Z*(P=C) form in a communication, but no details are provided.[78,79] In more recent work, Schoeller has only considered the *E*(P=C) isomer[80] as has Chernega.[81] The *E*(N=C) isomer has been calculated with B3LYP by Goumans et al. in a slightly different rotameric form.[82] By contrast, von Ragué-Schleyer has reported calculations on vinylphosphane (replacement of =NH with $=CH_2$) and finds that a pyramidal phosphorus is strongly preferred much as in our N=C isomers; however this system prefers the PH_2 unit to bisect the CCP plane in the *anti* conformation.[83] The barrier height to planarization for the vinyl phosphane at the MP4/6-31G(d) level of theory is 136.4 kJ/mol. The calculated rotational barrier around the C–P bond was only 2 kJ/mol, compared to 9 kJ/mol for the corresponding enamine. Our estimates for barriers to rotation are 89.2 kJ/mol for C–N rotation in the *P=C* isomer vs. 13.1 kJ/mol for P–C rotation in the *N=C* isomer

Research Article
doi.org/10.1002/ejic.202300495

Table 3. Geometries of the parent phospha(III)amidine model compounds;[a] numerals are distances in Å, letters are angles in °, keyed to the organizational diagram at right.

Parameter	*Z*(P=C)	Prasad[c]	*E*(P=C)	Schoeller[d]	Chernega[e]	Prasad[c]	*Z*(N=C)	*E*(N=C)	Goumans[f]
E [kJ mol^{-1}]	0[b]	0	+2.5[b]	–	–	+2.9	+22.1[b]	+22.5[b]	–
1	1.713	1.702	1.719	1.721	1.700	1.706	1.272	1.273	1.275
2	1.358	1.370	1.354	1.356	1.322	1.372	1.864	1.851	1.849
3	1.438	1.427	1.427	–	1.405	1.417	1.028	1.027	–
4	1.091	1.090	1.084	–	1.080	1.089	1.079	1.102	–
5	1.010	1.012	1.011	–	1.002	1.014	1.424	1.419	–
6	1.010	1.013	1.009	–	–	1.011	1.424	1.425	–
a	95.51	95.3	93.97	93.8	94.7	93.9	111.42	110.51	–
b	130.97	130.5	125.76	125.8	126.5	125.4	129.74	121.60	122.0
c	–	116.6	–	–	–	121.7	–	–	–
d	112.53	–	112.43		121.3	–	113.2	114.07	–
e	119.59	117.6	119.68	Forced flat		117.6	96.72	96.72	–
f	120.88	118.6	120.47	–	–	118.3	96.43	96.44	–
g	116.38	114.8	115.84	–	–	114.3	94.89	95.56	–
Σ(e–g)	356.9	351.0	356.0	–	–	350.2	288.0	288.7	–

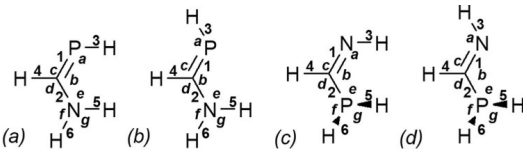

[a] B3LYP/6-31G(d). [b] B3LYP/6-311G++(3df,2pd). [c] Ref. [76]. [d] Ref. [80]. [e] Ref. [81]. [f] Ref. [82].

(non-optimized values, i.e. geometric relaxation was not allowed to take place.) Prasad obtains rotational barriers of 49.5 and 53.7 kJ/mol for the *E*(P=C) and *Z*(P=C) isomers,[76] respectively, while Wiberg calculates 49.4 and 50.9 kJ/mol for these parameters.[77]

We now consider the origins of the energetic preference for the aminophosphaalkene (P=C) over the phosphinoimine (N=C) in these model systems (which is directly relevant to **1a,b**, **2** and **3**). Figure 10 shows the orbital energies for all the filled and the lowest virtual orbitals of the four possible isomers and conformers. The most surprising feature of this diagram is that the frontier orbitals of the P=C isomers are considerably *destabilized* compared to those of N=C, even though the latter are the higher energy species. Indeed, it is not till the HOMO-6 is reached that the overall energetic preference switches to the more stable isomers (drawn as green-coloured levels in Figure 10). Thus the preference for *C*-amino-(σ^2,λ^3)-phosphaalkene over *C*-(σ^3,λ^3)-phosphinoimine is driven by the greater stabilization of σ(1) – σ(5) in the P=C form, i.e. the *s,p* σ-bonding orbitals of the molecular skeleton. These much more stable skeletal orbitals support the P=C tautomer's very high energy, electron-rich, frontier orbitals, namely *n*(P) and π(2). Thus for the *Z*(P=C) isomer these orbitals have energies of −5.5 and −7.3 vs. −6.8 and −7.8 eV for the corresponding *n*(P) and *n*(N) lone pair orbitals of the *Z*(N=C), while for *E*(P=C) vs. *E*(N=C) the numbers are −5.4, −7.1 vs. −6.9, −7.6 eV. We shall soon see that the topology of these frontier orbitals give *C*-amino-(σ^2,λ^3)-phosphaalkenes their unique properties, but it is very important to recognize that the π-delocalization that is observed in these structures does not drive the structural preference, but instead is supported by the bonding preferences of the skeletal σ orbitals.

Conceptual formation from fragments

To better understand the difference between the P=C and N=C, isomers we next contrast two orbital interaction diagrams, one between a simple phosphaalkene and an incoming NH_2 group, the other an imine interacting with PH_2. The relative energy of the *n*(P) lone pair and π(1) orbital of phosphaalkenes has been a subject of much debate; early computational studies tended to place the π orbital below the lone pair. Today, there is strong agreement among all the higher-level calculation methods, supported by UV-PES spectral data, that the order shown in Figure 11 is correct. This interaction (shown here only for the more stable *Z*(P=C) isomer) hardly affects the energy of *n*(P), which transfers into the aminophosphaalkene almost unchanged in energy or topology.

However, the interaction has profound consequences for π(1). Most of the overlap energy is taken away from the P=C bond to the newly formed *pseudo*-N=C bond which dominates the new π(1) MO. The newly created π(2) MO is weakly N=C antibonding and P=C bonding. The net π-bond order for both the N–C and C–P bonds is about 1.5. π(2) and π(3) are both pushed up in energy compared to π(1) and π(2) in H_2C=PH by

Research Article
doi.org/10.1002/ejic.202300495

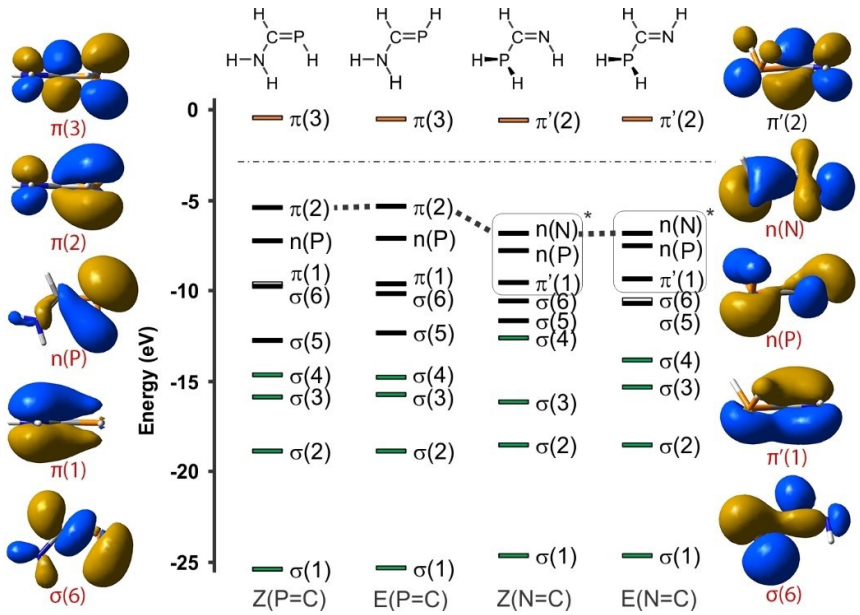

Figure 10. Energies of filled and first virtual orbitals of the *Z* and *E* parent aminophosphaalkenes and their phosphinoimine tautomers from B3LYP/6-311G++(3df,2pd) calculations. The latter are pyramidal at P so that the distinction between σ and π does not exist, but for ease of discussion the approximate designation π′ is used for the orbital that has N=C π-bonding character. Energies are ranked *Z*(P=C), 0 < *E*(P=C), +2.5 < *Z*(N=C), +22.1 < *E*(N=C), +22.5 kJ mol^{-1}. Kohn-Sham orbital isosurfaces of key FMOs of *Z*(P=C) are shown at left and of *Z*(N=C) at right.

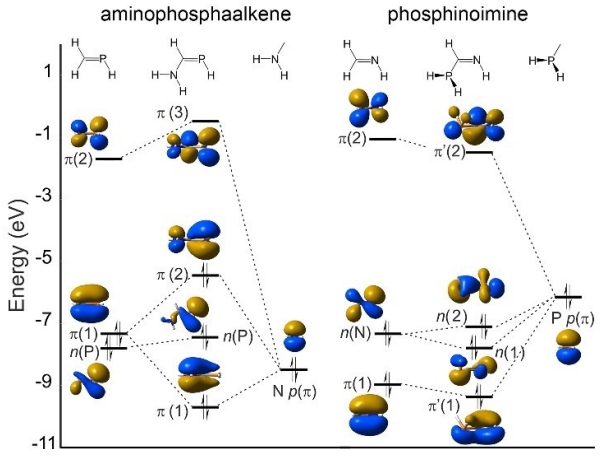

Figure 11. Orbital interaction diagrams conceptualizing the interactions of NH_2 with a P=C bond versus PH_2 with an N=C bond to generate the FMOs of the two isomers. Kohn-Sham MO surfaces are taken from B3LYP/6-311G++(3df,3pd) DFT calculations. Only π and *n* FMOs are considered.

over 1 eV, and the new π(2) is now an orbital strongly polarized towards P. However, the overall HOMO-LUMO gap is not expected to differ greatly from that in the parent phosphaalkene because π(3) is also raised significantly. For evidence supporting this notion, consider the lowest band in the electronic absorption spectrum of **1 a**: 28000 cm^{-1}, logε = 4.15, only slightly lower in energy than the value 30900 cm^{-1}, logε = 2.84 in MesP=CPh$_2$.[84] This band corresponds closely to the HOMO-LUMO transition, as verified by a TD-DFT calculation; for details, including the UV-vis spectrum of **1 a**, see the Supporting Information, especially Figure S24.

It is this π-charge drift that is responsible for the often-noted observation that aminophosphaalkenes have a "reversal of polarity" compared to simple phosphaalkenes.[63] The negative charge accumulation on carbon is most important when two amino groups are bound to C, i.e. in diaminophosphaalkenes (see below) but any electron donating substituent will have a similar effect. Weber has published extensive studies on the chemical reactivity of just such molecules and has conclusively demonstrated the chemical consequences of the π-reorganization represented by Figure 11. Much of this discussion was anticipated by the work of Chernega but in our opinion has not been sufficiently appreciated and bears repeating.[81]

It has been shown through a number of computational studies that aminophosphaalkenes will have unusually high barriers to rotation about the partial N–C π-bond. These barriers are higher than those in the nitrogen analogues (amidines) by 5–6 %, just as thioamides have higher barriers than amides.[77] This is another indicator that the overlap between the more compatible C and N orbitals of π-symmetry compete strongly with the P=C π-bond, as demonstrated in the orbital interaction diagram (Figure 11). We conclude that aminophosphaalkenes are non-innocent, strongly allylic electronic systems.

By contrast, in the phosphinoimine interaction diagram, the phosphorous *p*(π) interacts differently with the π(1) and *n*(N) FMOs of imine. By virtue of the out of plane rotated pyramidal phosphorus structure, the π′(1) delocalizes over the *n*(P) orbital and the π′(2) is somewhat stabilized; the HOMO-LUMO gap is only slightly smaller than in the parent imine. Significantly, the mixing of the (rotated) phosphorous *p*(π′) with the imine *n*(N)

Research Article
doi.org/10.1002/ejic.202300495

orbital induces two mixed lone-pair FMOs, labelled *n*(1) and *n*(2). The higher-lying combination represents primarily an enhanced imino *n*(N) donor, the HOMO of the phosphinoimine, whilst *n*(1) which has the larger P contribution is stabilized in the product.

Parent guanidines isomer preference

In contrast to the phospha(III)amidines, in monophospha(III)guanidines the parent compounds at the computed B3LYP/6-311G++(3df,3pd) level of theory are effectively equal-energy, so it is not surprising that in the fully substituted real molecule **4** the N=C choice becomes the lower-energy isomer. Thus, while *Z*(P=C) is the most stable, the (N=C) isomer is only about 3 kJ mol^{-1} higher in energy. The same basic picture obtains as when there is a single N atom attached to the central C atom: the HOMO-LUMO gap is considerably larger for the N=C isomers consistent with them being colourless compounds. The LUMO π(4) for the P=C isomer is an orbital with π symmetry and corresponds to the virtual C=P π* MO, and the HOMO π(3) is the typical polarized C=P with relatively low bond order. The π(2) MO is relatively non-bonding while π(1) is strongly polarized over the (formal) single bonded NCN moiety. The HOMO-1 has strong *n*(P) lone-pair character.

All of these FMOs are familiar from previous studies of diaminophosphaalkenes.[81] For the 'phosphinoamidine' (and here we consider only the lower energy *Z*(N=C) case, for which the FMO topologies are provided in Figure 12) the pyramidal geometry at the PH_2 unit destroys strict σ/π separation and the orbital topology mixes in a lot of P and single-bonded N character. The LUMO is σ(8) because the virtual π′ MO is driven to higher energy. The HOMO has π-like character for N-C-N with P(p) contribution and is a topological partner of the quite stable π′(1) in which the N-C-N in-phase π MO is strongly mixed with P. Similarly, π′(2) has strong P(p) contributions. Next are the closely spaced n(P) and n(N) lone-pair FMOs, of which the *former* is more stabilized due to the extensive mixing with the π′ orbitals, leaving the n(N) orbital as the stronger donor. A consideration of the orbital energies, as was done in Fig. 10, indicates that the energetic preference starts at σ(6) for (P=C), σ(7) for *Z*(N=C) and σ(6) for *E*(N=C) – indicated by the green shading in Figure 12. Once again, the high energy FMOs of the P=C isomer are sustained by the stronger bonding in the skeletal bonding orbitals.

Isomer Interconversion

A significant feature of this study is the tantalizing possibility of PH/NH tautomerism in some phospha(III)amidines. The large size of J_{PH} in the two species identified as *Z-anti*(N=C) and *E-syn*(N=C) is consistent with P(III)–H bonds; the chemical shift of the *Z-anti*(N=C) species is very similar to that reported for **2** (−84.3 ppm, J_{PH} = 251 Hz) and for **4** (−94.8 ppm, J_{PH} = 237 Hz) which are both *Z-anti*(N=C) in the solid state. The simultaneous presence of aminophosphaalkene and phosphinoimine isomers from a common source has been noted by other workers, but never explained or considered in detail.[62] The latter always remain the minor component in **1a**,**b**, while solvent changes

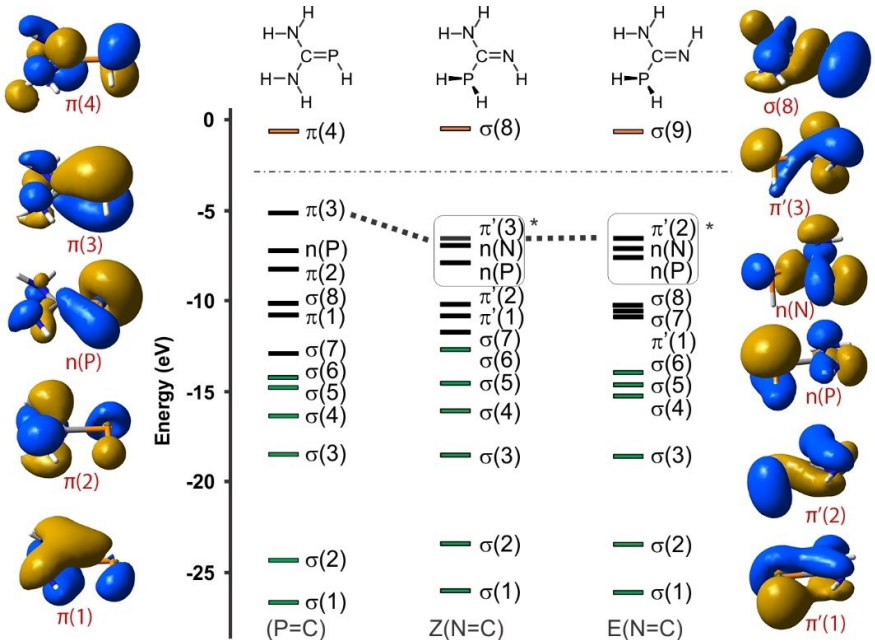

Figure 12. Energies of filled and first virtual orbitals from B3LYP/6-311++G(3df,3dp) calculations of model diaminophosphaalkene and *Z* and *E* phosphinoamidine isomers of monophospha(III)guanidines. The latter two are pyramidal at P so the distinction between σ and π does not exist, but for ease of discussion the approximate designation π′ is used for the orbitals that include N=C π-bonding character. Energies are ranked (P=C), 0 < *Z*(N=C), +3.2 < *E*(N=C), +12.1 kJ mol^{-1}. Kohn-Sham orbital isosurfaces of key FMOs of (P=C) are shown at left and of *Z*(N=C) at right.

Research Article
doi.org/10.1002/ejic.202300495

favour less *E-syn*(P=C) for low-polarity solvents (C_6D_6) or more in higher polarity ($CD_3(CO)CD_3$ and CD_3OD), in which the population of *E* and *Z* isomers reach parity).

Further insight into a possible role for the minor species was obtained with the ^{1}H EXSY NMR sequence (Scheme 5). This indicates *rapid* exchange between *Z-anti*(P=C) and what appears to be *E-syn*(N=C) (signals of this 1% constituent are significantly overlaid in the ^{1}H NMR) and slow exchange with *E-syn*(P=C). If this is the correct assignment, phosphinoimines could be vital links between the two aminophosphaalkene *E/Z* isomers based on an analogy to the enamine/imine exchange in organic chemistry (Scheme 6). Such an exchange is usually mediated by base (though both enamines and phosphaalkenes could act as the base in what become autocatalytic processes.)[85] As shown in Scheme 6, such tautomerism is poised for the exchange of *Z-anti* to *E-syn*. Notably, in the cases of **2** and **4**, which do not show tautomers in solution by NMR, *E/Z* isomers are also not detected.

Conclusions

If an exchangeable group at N or P is present – H or perhaps trimethylsilyl – then tautomerism between aminophospaalkenes and phosphinoimines becomes an open consideration. The question then becomes whether the tautomeric forms are usefully considered to be components of unified functional groups, i.e. as genuine "phospha(III)amidines" and "phospha(III)guanidines" in which trivalent phosphorus replaces trivalent nitrogen in the organic functional groups? This work supports an affirmative answer *by recognizing* their unique characteristics. Unlike the familiar all N cases, the mixed N,P tautomers are not degenerate and DFT calculations indicate a significant energetic preference for the P=C form in the parent monophospa(III)amidine and a smaller preference in monophospha(III)guanidines. Surprisingly, the 'real' organic-substituted compounds available for investigation show even closer energy balances, sometimes leading to an inversion in favour of the N=C isomers.

The detailed computational study presented here indicates that, whilst P=C π-bonding cannot compete on an even footing with N=C, the resultant lengthening of the P–C bond in the phosphinoimine tautomer facilitates rotation of the PR moiety such that the *n*(P) orbital – i.e. the lone pair – can overlap with the π-system. Evidently, this high polarizability at phosphorus restores some of the π-bonding energy and leads to a delocalized, and hence stabilized, π(1) FMO. This allows the phosphinoimine isomer to remain energetically in the game. Evidently, the substituents on the 'backbone' C atoms play critical roles. When these are an aromatic group, or hydrogen (in monophospha(III)formamidines), the aminophosphaalkene tautomer is preferred. However, when it is an electron donating group (such as ^{t}Bu in **2**, or an RNH group in **4**), the phosphinoimine tautomer is favoured. Further research on phospha(III)amidines and -guanidines substituted with ionizable substituents (PH, NHR or NH_2) may open up new avenues of reactivity for these hetero-element functional groups.

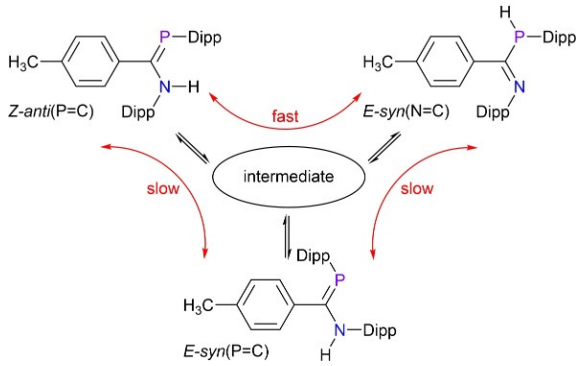

Scheme 5. Proposed solution exchange mechanism for **1 a** from EXSY NMR experiment.

Experimental Section

Materials and Methods. All experimental procedures were performed under a nitrogen atmosphere using modified Schlenk techniques. Solvents were reagent grade, or better, and used as received (methanol, ethanol, hexanes), distilled over $LiAlH_4$ (n-heptane) or distilled over sodium (xylenes). Infared spectra were recorded on Bomem MB-100 or Nicolet Avatar 360 spectrometers as KBr pellets or in a 0.1 mm NaCl solution cavity cell. ^{1}H, ^{13}C and ^{31}P NMR spectra were recorded on a Bruker AC250/Tecmag Macspect spectrometer operating at 250.13, 101.26 and 62.90 MHz, respectively, or a Varian Inova 500 operating at 499.3 (^{1}H), 202.1 (^{31}P), 125.6 (^{13}C), and 50.6 (^{15}N) MHz. ^{1}H NMR signals were referenced to tetramethylsilane, ^{13}C to $CDCl_3$, ^{13}P to an external H_3PO_4 sample and ^{15}N NMR to an external CH_3NO_2 sample. Mass spectra were undertaken in the Department of Chemistry, University of Alberta. Elemental analyses were run by MHW Laboratories, Phoenix, Az. DippN=C(*p*$CH_3C_6H_4$)Cl,[52] DippN=C(*p*$CH_3OC_6H_4$)Cl,[52] $DippPH_2$,[61] DippPHTMS,[61] ^{t}BuC(NPh)PPhTMS,[21c] ^{t}BuC(NDipp)PHDipp[41] and Dipp-N=C=N-Dipp[86] were prepared by the literature procedures.

Chemical Synthesis. *Synthesis of 1,3-bis(2,6-diisopropylphenyl)-2-(4-methylphenyl)-3-aza-1λ^3-phosphapropene (**1 a**).* To 38 mL of freeze-thaw degassed (5×) dry xylenes in a 250 mL side arm flask was added 5.00 g (15.9 mmol) of DippN=C(*p*$CH_3C_6H_4$)Cl and 3.10 g

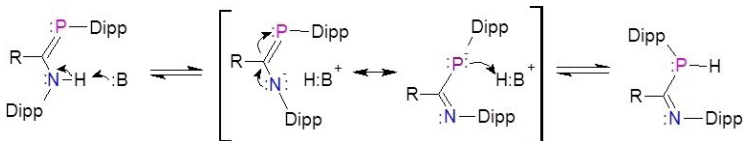

Scheme 6. Proposed mechanism for tautomerism exchanging *Z-anti*(P=C) for *E-syn*(N=C) isomers. Although a general base is drawn, the reaction would need to be autocatalytic in $CDCl_3$.

(15.9 mmol) $DippPH_2$. The flask was fitted with a reflux condenser and heated in a 200–215 °C oil bath. The reaction was monitored by ^{1}H NMR over four days, after which time all starting materials were consumed. Xylenes were removed under high vacuum. The remaining orange solid was dissolved in a minimum of hot 99% ethanol and cooled to −30 °C. After four days bright yellow crystals were filtered off and the filtrate was reduced to half the original volume. After harvesting a second crop, a total of 3.06 g (6.49 mmol) of crystals were obtained (41% yield). Analytical crystals were obtained by recrystallization from hot methanol, mp. 115–119 °C. Elemental Analysis: Calc. for $C_{32}H_{42}NP$: C, 81.49; H, 8.98; N, 2.97. Found: C, 81.57; H, 8.48; N, 3.02%. Mass spec (EI, 70 eV): *m/z* 471 (M^+, 23%); 428 (M–^{i}Pr, 100%); 278 (M–$C_6H_3{}^iPr_2H^+$, 81%); 176 ($C_6H_3{}^iPr_2NH^+$); 105 ($C_8H_9^+$, 20); 91 ($C_6H_5N^+$, 16). UV (methanol): λ_{max} 203 (ε 74 000), 232 (ε 24 500), 347 (ε 9 631). UV (n-hexane): λ_{max} 231 (ε 20 180), 272 (ε 11 217), 356 (ε 13 654). IR (KBr): νN–H 3351(vs); νP–H 2362(w). IR (CH_2Cl_2): νN–H 3350(m); νP–H 2360(m). IR (heptane): νN–H 3354(vs). ^{1}H NMR ($CDCl_3$): δ 0.81 (d, J(H–H) 6.7 Hz, 6H), 0.89 (d, J(H–H) 6.7 Hz, 6H), 1.26 (d, J(H–H) 6.7 Hz, 6H), 1.35 (d, J(H–H) 6.9 Hz, 6H), 2.22 (s, 3H), 3.00 (sept., J(H–H) 6.7 Hz, 2H), 3.84 (doublet of septets, J(H–H) 6.8 Hz, ^{4}J(P–H) 3.4 Hz, 2H), 6.23 (d, J(P–H) 2.4 Hz, 1H), 6.93–7.35 (mult., 10H). ^{13}C NMR ($CDCl_3$): δ 21.30, 22.48, 23.32, 25.44, 26.21, 26.24, 28.52, 33.24, 33.37, 123.27, 123.68, 127.09, 127.49, 127.74, 128.58, 128.69, 129.76, 134.63, 135.04, 135.34, 135.49, 135.56, 136.11, 138.50, 138.55, 144.96, 145.00, 154.12, 154.20, 186.02, 187.00. ^{31}P NMR ($CDCl_3$): δ −79.63 (minor isomer, d, J(P–H) = 241 Hz), −65.85 (minor isomer, d, J(P–H) = 241 Hz), 53.17 (minor isomer, s), 53.60 (major isomer, s), 54.78 (minor isomer, s), 54.96 (minor isomer, s), *and either*: 79.46 (minor isomer, s), 79.54 (minor isomer, s) *OR* 79.50 (minor isomer, d, ^{3}J(P–H) = 7.6 Hz). *Crystal Data* for $C_{34}H_{45}N_2P$ (M = 512.723 g/mol): monoclinic, space group Cc (no. 9), a = 10.475(3) Å, b = 17.439(4) Å, c = 17.029(4) Å, β = 100.320(2)°, V = 3060.4(13) Å^3, Z = 4, T = 173.15 K, μ(Mo Kα) = 0.113 mm^{-1}, D_{calc} = 1.113 g/cm^3, 20745 reflections measured (4.6° ≤ 2Θ ≤ 55.18°), 7050 unique (R_{int} = 0.0300, R_{sigma} = 0.0257) which were used in all calculations. The final R_1 was 0.0168 ($I \geq 2\sigma(I)$) and wR_2 was 0.0325 (all data).

*Synthesis of 1,3-bis(2,6-diisopropylphenyl)-2-(4-methoxyphenyl)-3-aza-1λ^3-phosphapropene (**1b**).* Prepared as for **1a** from 1.00 g (3.75 mmol) DipPHTMS **16** and 1.24 g (3.75 mmol) DippN=C-(*p*$CH_3OC_6H_4$)Cl **23** in 7 ml xylenes. Reaction was complete after overnight reflux. The yellow residue after removal of volatiles under vacuum were dissolved in a minimum of hot 99% EtOH and cooled to −30 °C to yield yellow nodules (0.724 g, 39.6% yield). Analytical and X-ray crystals were grown by the slow cooling of a hot MeOH solution to offer yellow block-like crystals, mp.: 133–136 °C. Mass spec (EI, 70 eV): *m/z* 487 (M^+, 12%); 444 (M–^{i}Pr, 69); 294 (M–$C_6H_3{}^iPr_2H^+$, 100); 176 ($C_6H_3{}^iPr_2NH^+$,11); 135 (C_8H_9NO, 34); 121 ($C_8H_9O^+$, 21); 91 ($C_6H_5N^+$, 11); 77 ($C_6H_5^+$, 6.8). UV(methanol): λ_{max} 204 (ε 303 847); 275 nm (ε 28 603); 327 nm (ε 33 761). Elemental Analysis: Calc. for $C_{32}H_{42}NOP$: C, 78.81; H, 8.68; N, 2.87. Found: C, 76.07; H, 7.58; N, 2.80%. UV(methanol): λ_{max} 204 (ε 303 847); 275 nm (ε 28 603); 327 nm (ε 33 761). ^{1}H NMR ($CDCl_3$): δ 0.83 (d, J(H–H) 6.9 Hz, 6H), 0.92 (d, J(H–H) 6.9 Hz, 6H), 1.27 (d, J(H–H) 6.7 Hz, 6H), 1.36 (d, J(H–H) 6.9 Hz, 6H), 3.00 (sept., J(H–H) 6.7 Hz, 2H), 3.70 (s, 3H), 3.85 (doublet of septets, J(H–H) 6.7 Hz, ^{4}J(P–H) 3.4 Hz, 2H), 6.24 (d, J(P–H) 2.4 Hz, 1H), 6.63-7.35 (mult., 10H). ^{13}C NMR ($CDCl_3$): δ 22.53, 23.30, 25.43, 26.21, 26.24, 28.54, 33.23, 33.35, 55.44, 113.44, 123.24, 123.70, 127.12, 128.90, 129.16, 129.73,130.16, 130.58, 135.34, 135.46, 135.53, 136.11, 144.95, 144.98, 154.10, 154.18, 160.28, 160.33, 185.65, 186.64. ^{31}P NMR ($CDCl_3$, ^{1}H coupled): δ −80.30 ppm (minor isomer, d, J_{P-H} = 241 Hz), 51.38 (major isomer, s), 52.55 (minor isomer, s), 79.03 (minor isomer, s). *Crystal Data* for $C_{32}H_{42}NOP$ (M = 487.670 g/mol): monoclinic, space group $P2_1/c$ (no. 14), a = 17.9798(13) Å, b = 10.0150(7) Å, c = 17.9976(13) Å, β = 116.903(1)°, V = 2890.0(4) Å^3, Z = 4, T = 173(2) K, μ(Mo Kα) = 0.119 mm^{-1}, D_{calc} = 1.121 g/cm^3, 41115 reflections measured (4.54° ≤ 2Θ ≤ 55.1°), 6641 unique (R_{int} = 0.0478, R_{sigma} = 0.0340) which were used in all calculations. The final R_1 was 0.0337 ($I \geq 2\sigma(I)$) and wR_2 was 0.0673 (all data).

*Synthesis of N-(2,2-dimethyl-1-(2,6-diisopropylphenyl-phosphino)propylidene)aniline (**2**).* *n*-butyl lithium (2.2 mL, 1.6 M) was added into a solution of $DippPH_2$ (0.65 g, 3.33 mmol) and tetrahydrofuran (7.5 mL) in −60 °C and was stirred for 30 min. The mixture was allowed to warm to RT. DippN=C(^{t}Bu)Cl (0.93 g, 3.33 mmol) was added to the solution at −60 °C and the mixture was allowed to warm to RT and stirred overnight. Solvent was removed with vacuum line and the residue was washed with hexane to precipitate LiCl. Crude product was recrystallized from 15 mL methanol to give colorless crystals. Yield: 1.05 g, 72%. ^{1}H NMR ($CDCl_3$): δ 1.06 (d, 3H, $CH(CH_3)_2$), 1.10 (d, 6 H, $CH(CH_3)_2$), 1.16 (d, 3H, $CH(CH_3)_2$), 1.20 (d, 6H, $CH(CH_3)_2$), 1.20 (s, 9H, $C(CH_3)_3$), 1.22 (d, 3H, $CH(CH_3)_2$), 1.37 (d, 3H,$CH(CH_3)_2$), 2.79 (sept, 1H, $CH(CH_3)_2$), 2.93 (sept, 1H, $CH(CH_3)_2$), 3.55 (sept, 2H, $CH(CH_3)_2$), 4.74 (d, 1H, PH), 6.99 (t, 1H, p-Dipp), 7.01 (d, 2H, m-Dipp), 7.03 (d, 2H, m-Dipp), 7.09 (d, 4H, m-Dipp), 7.30 (t, 1H, p-Dipp). ^{31}P NMR ($CDCl_3$): δ −84.73 (d, J(P–H) = 251.26). ^{13}C NMR ($CDCl_3$): δ 21.65 (CH_3 of iso-pr), 21.70 (CH_3 of iso-pr), 23.49 (CH_3 of iso-pr), 27.03 (CH_3 of iso-pr), 28.32 ($CH(CH_3)_2$), 28.77 ($CH(CH_3)_2$), 29.30 (CH_3 of ^{t}Bu), 33.63 ($CH(CH_3)_2$), 45.32 ($C(CH_3)_3$), 122.70 (m-Dipp-N), 123.03 (m-Dipp-N), 123.33 (p-Dipp- N), 123.36 (m-Dipp-N), 128.62 (ipso-Dipp-P), 130.78 (p-Dipp-P), 134.53 (o-Dipp-N), 134.89 (o-Dipp-N), 146.64 (ipso-Dipp-N), 154.59 (o-Dipp-P), 182.21 (C=N). Elemental Analysis: Calc. for $C_{29}H_{44}NP$: C, 79.59; H, 10.13; N, 3.20. Found: C, 79.30; H, 10.16; N, 3.65. Pure colorless crystals grew from methanol at −25 °C under N_2 and crystallographic data was determined at −100 °C. *Crystal Data* for $C_{29}H_{44}NP$ (M = 437.653 g/mol): monoclinic, space group $P2_1/c$ (no. 14), a = 11.649(3) Å, b = 25.508(6) Å, c = 9.885(2) Å, β = 111.027(3)°, V = 2741.6(11) Å^3, Z = 4, T = 173.15 K, μ(Mo Kα) = 0.115 mm^{-1}, D_{calc} = 1.060 g/cm^3, 39414 reflections measured (3.74° ≤ 2Θ ≤ 50.5°), 4953 unique (R_{int} = 0.0846, R_{sigma} = 0.0643) which were used in all calculations. The final R_1 was 0.0359 ($I \geq 2\sigma(I)$) and wR_2 was 0.0567 (all data).

*Synthesis of (2,6-Diisopropylphenyl)[bis(2,6-diisopropylphenylamino)methylidene]-phosphane (**4**).* In a 250 ml side arm flask, 3.22 g (16.6 mmol) of $DippPH_2$ and 60 ml dry THF were combined and cooled to 0 °C. 8.36 ml (2.5% excess) of 2 M ^{n}BuLi was then added, resulting in a dark orange solution, stirred for another 10 min and allowed to warm to RT. After cooling again to 0 °C, 6.0 g (16.6 mmol) of Dipp-N=C=N-Dipp in 35 ml dry THF was added dropwise. After refluxing 2 h, the cooled mixture is quenched with 2 ml H_2O, dried with anhydrous $MgSO_4$, filtered and all volatiles removed. The residue was dissolved in a minimum volume of hot 99% ethanol and cooled to −30 °C. Two harvests provided 3.508 g of lightly coloured solid (38% yield). Analytical crystals were obtained from a second recrystallization; mp. 135–139 °C. ^{1}H NMR ($CDCl_3$): δ 1.00(d, J(H–H) 6.7 Hz, 6H), 1.06(d, J(H–H) 6.7 Hz, 6H), approx. 1.21(s, 12H), 1.36(d, J(H–H) 6.9 Hz, 6H), 1.42(d, J(H–H) 6.9 Hz, 6H), 3.17(sept., J(H–H) 6.9 Hz, 2H), approx. 3.20 (hidden under other septet)(s, 2H), 3.61(broad s, 2H), 4.87(d, J(P–H) 237 Hz, 1H), 5.35(s, 1H), 7.04–7.41(m, 9H). ^{13}C NMR ($CDCl_3$): δ 22.97, 23.28, 23.47, 23.59, 23.79, 23.91, 24.08, 24.38, 24.65, 24.94, 25.22, 27.88, 27.99, 28.35, 28.45, 28.73, 29.20, 33.30, 33.50, 33.79, 33.99, 122.42, 122.88, 123.03, 123.32, 123.81, 124.27, 126.77, 127.12, 127.34, 128.31, 130.76, 131.74, 134.37, 139.33, 139.62, 146.01, 146.18, 146.67, 154.36, 156.52, 157.09. ^{31}P NMR ($CDCl_3$): δ −94.82 ppm (d, J(H–P) 237 Hz). *Crystal Data* for $C_{37}H_{53}N_2P$ (M = 556.820 g/mol): monoclinic, space group $P2_1/n$ (no. 14), a = 11.7121(13) Å, b = 18.524(2) Å, c = 15.5663(17) Å, β = 90.697(1)°, V = 3377.0(6) Å^3, Z = 4, T = 173.15 K, μ(Mo Kα) = 0.108 mm^{-1}, D_{calc} = 1.095 g/cm^3, 49726 reflections measured (3.42° ≤ 2Θ ≤ 56.22°), 8181

unique (R_{int} = 0.0460, R_{sigma} = 0.0347) which were used in all calculations. The final R_1 was 0.0293 ($I \geq 2\sigma(I)$) and wR_2 was 0.0507 (all data).

Solid State NMR. The solid-state ^{31}P CP-MAS NMR spectra were acquired on a 500 MHz Varian Unity INOVA spectrometer using a Varian 4 mm HFXY T3 probe operating under ambient temperature and an MAS rate of 10 or 15 kHz. A zirconium oxide rotor with a vespel drive and end cap was used. Spectral referencing was carried out with 85% phosphoric acid as the primary reference (δ_p = 0 ppm). The spectra were acquired using a 5 s recycle delay, a sweep width of 500 kHz (dwell time of 2 μs), an acquisition time of 100 ms, and a 2.5 μs π/2 pulse width on proton. Cross-polarization (CP) was carried out from the ^{1}H to the ^{31}P nucleus using the ramped CP method with a contact time of 1.5 ms and a B_1 field strength of 83.33 kHz. Two pulse phase modulated (TPPM) decoupling using a B_1 field strength of 100 kHz was applied to the ^{1}H nucleus during the acquisition period.

DFT Computational Methods. The geometries obtained from the SC-XRD HAR (ignoring any minor components from disorders) were optimised in the gas phase using the well-known B3LYP functional[87,88] and the 6–31 + G(d,p) basis set. NPA charges were calculated using normal bond order analysis. Minimum geometries were verified using harmonic vibrational analysis. The use of Grimme's D3 correction for dispersion, an attractive effect which is not readily accounted for by the bare B3LYP functional, was also applied and the results contrasted with non-corrected results.[74,75,89] All calculations were performed using Gaussian 16 W on an AMD Ryzen Threadripper 16-core 3.75 Hz PC under Windows 10 or on a regional computational cluster.[90]

Supporting Information

(See footnote on the first page of this article): chemical reactivity, voltammetry and interpretation for **1a**, full X-ray crystallographic experimental and detailed structure and refinement descriptions, NMR data and interpretation, Infrared spectra and assignments. UV-vis spectroscopy and TD-DFT assignments. Additional DFT computational results.

Deposition Numbers 2285832-2285839 contain the supplementary crystallographic data for this paper. These data are provided free of charge by the joint Cambridge Crystallographic Data Centre and Fachinformationszentrum Karlsruhe Access Structures service. The authors have cited additional references within the Supporting Information.[91–110]

Acknowledgements

The authors gratefully acknowledge financial support from the Natural Sciences and Engineering Research Council (Canada), the University of Lethbridge (R.T.B.) and Saint Mary's University (J.D.M). Guanging Lin, Tony Montina and Michael P. Opyr are thanked for the solid-state NMR spectroscopic measurements. This research was enabled in part by support provided by ACENET (https://ace-net.ca/) and the Digital Research Alliance of Canada (alliancecan.ca).

Conflict of Interests

The authors declare no conflict of interest.

Data Availability Statement

The data that support the findings of this study are available in the supplementary material of this article.

Keywords: aminophosphaalkenes · computational chemistry · isomerism · phosphinoimine · Hirshfeld atom refinement

[1] a) K. Dimroth, P. Hoffmann, *Angew. Chem. Int. Ed.* **1964**, *3*, 384; b) K. Dimroth, P. Hoffmann, *Chem. Ber.* **1966**, *99*, 1325–1331; c) R. Allmann, *Chem. Ber.* **1966**, *99*, 1332–1340; d) K. Dimroth, *Top. Curr. Chem.* **1973**, *38*, 1–147.
[2] For some reviews, see: a) T. Sasamori, V. Lee, N. Nagahora, S. Morisako in *Comprehensive Inorganic Chemistry III*, (Ed.: R. Laitinen), Elsevier, Oxford, **2023**, pp. 118–164; b) J. D. Protasiewicz in *Comprehensive Inorganic Chemistry II*, Vol. 1 (Eds.: J. Reedijk, K. Poeplemeier), Elsevier, Oxford, **2013**, pp. 325–348; c) M. Yoshifuji, *Molecules* **2022**, *27*, 1557; d) L. Weber, F. Ebeler, R. S. Ghadwal, *Coord. Chem. Rev.* **2022**, *461*, 214499; e) K. Ota, R. Kinjo, *Chem. Soc. Rev.* **2021**, *50*, 10594–10673; f) L. Dostal, *Coord. Chem. Rev.* **2017**, *353*, 142–158; g) R. C. Fischer, P. P. Power, *Chem. Rev.* **2010**, *110*, 3877–3923; h) R. Waterman, *Dalton Trans.* **2009**, 18–26; i) D. P. Gates, *Top. Curr. Chem.* **2005**, *250*, 107–126; j) L. Weber, *Angew. Chem. Int. Ed.* **2002**, *41*, 563–572; k) P. P. Power, *Chem. Rev.* **1999**, *99*, 3463–3503; l) N. C. Norman, *Polyhedron* **1993**, *12*, 2431–2446; m) F. Mathey, A. Marinetti, S. Bauer, P. Le Floch, *Pure Appl. Chem.* **1991**, *63*, 856–858; n) A. N. Chernega, M. Yu. Antipin, Yu. T. Struchov, *J. Struct. Chem. USSR* **1988**, *29*, 265–303.
[3] A. M. Priegert, B. W. Rawe, S. C. Serin, D. P. Gates, *Chem. Soc. Rev.* **2016**, *45*, 922–953.
[4] K. Esfandiarfard, A. I. Arkhypchuk, A. Orthaber, S. Ott, *ChemPlusChem* **2023**, *88*, e202300067.
[5] M. A. Shameem, A. Orthaber, *Chem. Eur. J.* **2016**, *22*, 10718–10735.
[6] D. M. Seth Jr., R. Waterman, *Organometallics* **2023**, *42*, 1213–1219.
[7] P. Royla, K. Schwedtmann, Z. Han, J. Fidelius, D. P. Gates, R. M. Gomila, A. Frontera, J. J. Weigand, *J. Am. Chem. Soc.* **2023**, *145*, 10364–10375.
[8] A. Merschel, Y. V. Vishnevskiy, B. Neumann, H.-G. Stammler, R. S. Ghadwal, *Dalton Trans.* **2022**, *51*, 8217–8222.
[9] A. M. Camelio, A. Krasovskiy, B. Bailey, A. Davis, *J. Org. Chem.* **2022**, *87*, 2022–2044.
[10] S. Wang, T. Li, Y. Heng, G. Hou, G. Zi, M. D. Walter, *Organometallics* **2021**, *40*, 2149–2165.
[11] D. Wang, S. Wang, G. Hou, G. Zi, M. D. Walter, *Inorg. Chem.* **2020**, *59*, 14549–14563.
[12] C. Zhang, G. Hou, G. Zi, W. Ding, M. D. Walter, *Inorg. Chem.* **2019**, *58*, 1571–1590.
[13] C. Zhang, G. Hou, G. Zi, W. Ding, M. D. Walter, *J. Am. Chem. Soc.* **2018**, *140*, 14511–14525.
[14] M. Fischer, C. Hering-Junghans, *Chem. Sci.* **2021**, *12*, 10279–10289.
[15] A. G. Baradzenka, M. Pilkington, A. Dmitrienko, G. I. Nikonov, *Chem. Eur. J.* **2023**, *29*, e202300523.
[16] T. van Dijk, S. Burck, M. K. Rong, A. J. Rosenthal, M. Nieger, J. C. Slootweg, K. Lammertsma, *Angew. Chem. Int. Ed.* **2014**, *53*, 9068–9071.
[17] R. Streubel, H. Wilkens, P. G. Jones, *Chem. Eur. J.* **2000**, *6*, 3997–4000.
[18] C. R. Groom, I. J. Bruno, M. P. Lightfoot, S. C. Ward, *Acta Crystallogr.* **2016**, B*72*, 171–179.
[19] The magnificent diversity that phosphorus imparts to multiple-bond chemistry makes nomenclature challenging: P(V) can participate via ylidic bonds to C and other elements, which are sometimes included in discussions of double bonding; they are excluded here. The term "phosphamidine" (with a single "a") has been used in the past by Soviet researchers to describe amino-imino substitution of phosphoric acid derivatives. This is an example of the isolobality of $R_2P(V)$ and RC(IV), e.g. similar to the formal analogy that exists between phosphazenes and azines; see A. Steiner, S. Zacchini, P. I. Richards, *Coord. Chem. Rev.* **2002**, *227*, 193–216. For a recent example of similar,

but not consistent, usage: N. Nebra, C. Lescot, P. Dauban, S. Mallet-Ladeira, *Eur. J. Org. Chem.* **2013**, 984–990. Here we are concerned with the replacement of *nitrogen*, not carbon, and P(III) not P(V). The argument of this paper will be that the analogy between P(III) and nitrogen in (organic) amidine and guanidine functional groups is fruitful and worth supporting. The usages phoshaamidine (with two "a"), or phospha(III)amidine, and phosphaguanidine, or phospha(III)guanidine, have gained considerable support in the literature for this scenario. However, *Science of Synthesis* (a.k.a. *Houben-Weil*) restricts the latter term to compounds containing R_2P–C moieties, a position we argue against: T. L. Gilchrist, *Sci. Synth.* **2005**, *18*, 1117.

[20] a) P. Le Floch, *Coord. Chem. Rev.* **2006**, *250*, 627–681; b) L. Weber, *Eur. J. Inorg. Chem.* **2000**, 2425–2441; J. Grobe, D. Le Van, *J. Fluorine Chem.* **2004**, *125*, 801–821.

[21] a) K. Issleib, O. Löw, *Z. Anorg. Allg. Chem.* **1966**, *346*, 241–254; b) K. Issleib, H. Schmidt, H. Meyer, *J. Organomet. Chem.* **1978**, *160*, 47-57; c) K. Issleib, H. Schmidt, H. Meyer, *J. Organomet. Chem.* **1980**, *192*, 33–9; d) K. Issleib, H. Schmidt, C. Wirkner, *Synth. React. Inorg. Met.-Org. Chem.* **1981**, *11*, 279–285; e) A. Schmidpeter, W. Gebler, F. Zwaschka, W. S. Sheldrick, *Angew. Chem. Int. Ed.* **1980**, *19*, 722–723; f) K. Issleib, E. Leissring, M. Riemer, H. Oehme, *Z. Chem.* **1983**, *23*, 99–100; g) A. N. Chernega, M. Yu. Antipin, Yu. T. Struchkov, T. V. Sarina, V. D. Romanenko, *Russ. J. Struct. Chem.* **1986**, *27*, 122; h) A. N. Chernega, A. V. Ruban, V. D. Romanenko, L. N. Markovski, A. A. Korkin, M. Yu. Antipin, Yu. T. Struchkov, *Heteroat. Chem.* **1991**, *2*, 229–2418e; i) E. Fuchs, F. Krebs, H. Heydt, M. Regitz, *Tetrahedron* **1994**, *50*, 759-774.

[22] A. J. Roering, L. T. Elrod, J. K. Pagano, S. L. Guillot, S. M. Chan, J. M. Tanskib, R. Waterman, *Dalton Trans.* **2013**, *42*, 1159–1167.

[23] S. T. Liddle, K. Izod, *Organometallics* **2004**, *23*, 5550-.

[24] N. E. Mansfield, J. Grundy, M. P. Coles, A. G. Avent, P. B. Hitchcock, *J. Am. Chem. Soc.* **2006**, *128*, 13879–13893.

[25] R. Appel, F. Knoch, B. Laubach, R. Sievers, *Chem. Ber.* **1983**, *116*, 1873–1879.

[26] A. K. Adhikari, T. Grell, P. Lonnecke, E. Hey-Hawkins, *Eur. J. Inorg. Chem.* **2017**, 5329–5333.

[27] A. Surana, S. Singh, R. K. Bansal, N. Peulecke, A. Spannenberg, J. Heinicke, *J. Organomet. Chem.* **2002**, *646*, 113–124.

[28] A. J. Arduengo III, C. J. Carmalt, J. A. C. Clyburne, A. H. Cowley, R. Pyati, *Chem. Commun.* **1997**, 981–982.

[29] A. J. Arduengo III, J. C. Calabrese, A. H. Cowley, H. V. R. Dias, J. R. Goerlich, W. J. Marshall, B. Riegel, *Inorg. Chem.* **1997**, *36*, 2151–2158.

[30] G. D. Frey, M. Song, J.-B. Bourg, B. Donnadieu, M. Soleilhavoup, G. Bertrand, *Chem. Commun.* **2008**, 4711–4713.

[31] M. Melaimi, M. Soleilhavoup, G. Bertrand, *Angew. Chem. Int. Ed.* **2010**, *49*, 8810–8849.

[32] P. Rosa, C. Goverd, G. Bernardinelli, T. Berclaz, M. Geoffroy, *J. Phys. Chem. A* **2003**, *107*, 4883–4892.

[33] N. E. Mansfield, J. Grundy, M. P. Coles, P. B. Hitchcock, *Polyhedron* **2010**, *29*, 2481–2488.

[34] N. E. Mansfield, M. P. Coles, P. B. Hitchcock, *Polyhedron* **2012**, *37*, 9–13.

[35] H. Schmidbaur, U. Deschler, B. Milewski-Mahrla, *Chem. Ber.* **1983**, *116*, 1393–1402.

[36] E. J. Fernandez, M. C. Gimeno, P. G. Jones, B. Ahrens, A. Laguna, M. Laguna, J. M. L. de Luzuriaga, *J. Chem. Soc. Dalton Trans.* **1994**, 3487–3492.

[37] M. Nieger, R. Appel, V. Winkhaus, *CSD Communication* **1998**, refcode: NURZAB.

[38] K. Paasch, M. Nieger, E. Niecke, *Angew. Chem. Int. Ed.* **1995**, *34*, 2369–2371.

[39] M. Nieger, E. Niecke, K. Paasch, *CSD Communication* **2009**, refcode: CALLIM.

[40] M. Song, B. Donnadieu, M. Soleilhavoup, G. Bertrand, *Chem. Asian J.* **2007**, *2*, 904–908.

[41] X. Li, H. Song, C. Cui, *Dalton Trans.* **2009**, 9728–9730.

[42] a) F. T. Edelmann, *Adv. Organomet. Chem.* **2008**, *57*, 193–352; b) J. Barker, M. Kilner, *Coord. Chem. Rev.* **1994**, *133*, 219-.

[43] M. P. Coles, *Dalton Trans.* **2006**, 985–1001.

[44] R. Kandel, K. Huynh, L. Dalgliesh, R. Wang, P. G. Jessop, *Inorg. Chim. Acta* **2016**, *445*, 117–123.

[45] R. Kandel, G. Schatte, L. Laverdure, N. Mosey, P. G. Jessop, *Can. J. Chem.* **2021**, *99*, 277–285.

[46] M. K. Rong, F. Holtrop, J. C. Slootweg, K. Lammertsma, *Coord. Chem. Rev.* **2019**, *382*, 57–68.

[47] A. J. Roering, S. E. Leshinski, S. M. Chan, T. Shalumova, S. N. MacMillan, J. M. Tanski, R. Waterman, *Organometallics* **2010**, *29*, 2557–2565.

[48] L. Weber, *Coord. Chem. Rev.* **2005**, *249*, 741–763.

[49] *The chemistry of the amidines and imidates*, *Vols. 1 & 2* (Eds.: S. Patai, Z. Rappoport), Wiley, Chichester, **1991**.

[50] R. T. Boeré, M. L. Cole, P. C. Junk, J. D. Masuda, G. Wolmershäuser, *Chem. Commun.* **2004**, 2564-2565.

[51] J. D. Masuda, R. T. Boeré, *Dalton Trans.* **2016**, 2102–2115.

[52] R. T. Boeré, V. Klassen, G. Wolmershäuser, *J. Chem. Soc. Dalton Trans.* **1998**, 4147–4154.

[53] R. E. Boeré, R. T. Boeré, J. Masuda, G. Wolmershäuser, *Can. J. Chem.* **2000**, *78*, 1613–1619.

[54] J. Grundy, M. P. Coles, P. B. Hitchcock, *Dalton Trans.* **2003**, 2573–2577.

[55] This structure can thus be equally well described as a phospha(III)amidine in the N=C tautomeric form which bears an electron-rich secondary amino group as the "backbone" substituent. Alternatively, it can be described as an *E-syn N,N'*-amidine bearing a DippPH substituent at C1; such ambiguity in description is, of course, typical of guanidines.

[56] F. Kleemiss, O. V. Dolomanov, M. Bodensteiner, N. Peyerimhoff, L. Midgley, L. J. Bourhis, A. Genoni, L. A. Malaspina, D. Jayatilaka, J. L. Spencer, F. White, B. Grundkötter-Stock, S. Steinhauer, D. Lentz, H. Puschmann, S. Grabowsky, *Chem. Sci.* **2021**, *12*, 1675–1692.

[57] M. Woińska, S. Grabowsky, P. M. Dominiak, K. Woźniak, D. Jayatilaka, *Sci. Adv.* **2016**, *2*, e1600192.

[58] G. Häfelinger, K. H. Kuske in *The chemistry of the amidines and imidates, Vol. 2* (Eds.: S. Patai, Z. Rappoport), Wiley, Chichester, **1991**, chap. 1, pp. 1–100.

[59] R. T. Boeré, V. Klassen, G. Wolmershäuser, *Can. J. Chem.* **2000**, *78*, 583–589.

[60] Other synthetic approaches include the addition of an anionic C or hydride to monophosphacarbodiimides,[13] or the addition of secondary phosphanes to nitrilium ions (ref.[15] and T. van Dijk, S. Burck, A. J. Rosenthal, M. Nieger, A. W. Ehlers, J. C. Slootweg, K. Lammertsma, *Chem. Eur. J.* **2015**, *21*, 9328–9331). However, when imidoyl chlorides are isolable, this method remains much more affordable and very easily scaled to large quantities.

[61] R. T. Boeré, J. D. Masuda, *Can. J. Chem.* **2002**, *80*, 1607–1617.

[62] S. C. Rathnayaka, S. V. Lindeman, N. P. Mankad, *Inorg. Chem.* **2018**, *57*, 9439–9445.

[63] L. Weber, *Eur. J. Inorg. Chem.* **2000**, 2425–2441.

[64] O. Mundt, G. Becker, W. Uhl, W. Massa, M. Birkhahn, *Z. Anorg. Allg. Chem.* **1986**, *540*, 319-335.

[65] This structure was also reported by van Dijk et al., ref. [16] (CSD refcode: XOPBAH) but the structure model was refined using the IAM, making direct comparisons less useful here.

[66] S. T. Liddle, K. Izod, *Chem. Commun.* **2003**, 772–223.

[67] R. T. Boeré, *ACS Omega* **2018**, *3*, 18170–18180.

[68] D. Biskup, G. Schnakenburg, R. T. Boeré, A. Espinosa Ferao, R. K. Streubel, *Nat. Chem.*, in press.

[69] G. Jin, C. Jones, P. C. Junk, K.-A. Lippert, R. P. Roseab, A. Stasch, *New J. Chem.* **2009**, *33*, 64–75.

[70] T. Krachko, M. Bispinghoff, A. M. Tondreau, D. Stein, M. Baker, A. W. Ehlers, J. C. Slootweg, H. Grützmacher, *Angew. Chem. Int. Ed.* **2017**, *56*, 7948–7951.

[71] A. Ecker, U. Schmidt, *Chem. Ber.* **1973**, *106*, 1453–1458.

[72] M. Yoshifuji, K. Toyota, N. Inamoto, *Tetrahedron Lett.* **1985**, *26*, 1727–1730.

[73] R. T. Boeré, J. D. Masuda, *Acta Crystallogr. Sect. E* **2011**, *67*, m895–m896.

[74] a) S. Grimme, J. Antony, S. Ehrlich, H. Krieg, *J. Chem. Phys.* **2010**, *132*, 154104; b) L. Goerigk, S. Grimme, *Phys. Chem. Chem. Phys.* **2011**, *13*, 6670–6688.

[75] E. R. Johnson, A. D. Becke, *J. Chem. Phys.* **2006**, *124*, 174104.

[76] B. V. Prasad, G. Grover, P. Uppal, D. Kaur, *J. Mol. Struct.* **1999**, *458*, 227–237.

[77] K. B. Wiberg, P. R. Rablen, *J. Am. Chem. Soc.* **1995**, *117*, 2201–2209.

[78] W. W. Schoeller, *J. Chem. Soc. Chem. Commun.* **1982**, 569–570.

[79] W. W. Schoeller, *J. Chem. Soc. Chem. Commun.* **1985**, 334–335.

[80] L. Weber, S. Uthmann, H.-G. Stammler, B. Neumann, W. W. Schoeller, R. Boese, D. Bläser, *Eur. J. Inorg. Chem.* **1999**, 2369–2381.

[81] A. N. Chernega, A. V. Ruban, V. D. Romanenko, L. N. Markovski, A. A. Korkin, M. Yu. Antipin, Y. T. Struchkov, *Heteroat. Chem.* **1991**, *2*, 229–241.

[82] T. P. M. Goumans, A. W. Ehlers, M. J. M. Vlaar, S. J. Strand, K. Lammertsma, *J. Organomet. Chem.* **2002**, *643–644*, 369–375.
[83] C. Schade, P. von Ragué Schleyer, *Chem. Commun.* **1987**, 1399–1401.
[84] Th. C. Klebach, R. Lourens, F. Bickelhaupt, *J. Am. Chem. Soc.* **1978**, *100*, 4886–4888.
[85] Z. Rappoport, *The Chemistry of Enamines*, Wiley, New Jersey, USA, **1994**.
[86] G. Himbert, W. Schwickerath, *Liebigs Ann. Chem.* **1984**, 85-97.
[87] A. D. Becke, *J. Chem. Phys.* **1993**, *98*, 5648.
[88] C. Lee, W. Yang, R. G. Parr, *Phys. Rev. B* **1988**, *37*, 785.
[89] J. Antony, S. Grimme, *Phys. Chem. Chem. Phys.* **2006**, *8*, 5287–5293.
[90] Gaussian 16, Revision C.01, M. J. Frisch, G. W. Trucks, H. B. Schlegel, G. E. Scuseria, M. A. Robb, J. R. Cheeseman, G. Scalmani, V. Barone, G. A. Petersson, H. Nakatsuji, X. Li, M. Caricato, A. V. Marenich, J. Bloino, B. G. Janesko, R. Gomperts, B. Mennucci, H. P. Hratchian, J. V. Ortiz, A. F. Izmaylov, J. L. Sonnenberg, D. Williams-Young, F. Ding, F. Lipparini, F. Egidi, J. Goings, B. Peng, A. Petrone, T. Henderson, D. Ranasinghe, V. G. Zakrzewski, J. Gao, N. Rega, G. Zheng, W. Liang, M. Hada, M. Ehara, K. Toyota, R. Fukuda, J. Hasegawa, M. Ishida, T. Nakajima, Y. Honda, O. Kitao, H. Nakai, T. Vreven, K. Throssell, J. A. Montgomery, Jr., J. E. Peralta, F. Ogliaro, M. J. Bearpark, J. J. Heyd, E. N. Brothers, K. N. Kudin, V. N. Staroverov, T. A. Keith, R. Kobayashi, J. Normand, K. Raghavachari, A. P. Rendell, J. C. Burant, S. S. Iyengar, J. Tomasi, M. Cossi, J. M. Millam, M. Klene, C. Adamo, R. Cammi, J. W. Ochterski, R. L. Martin, K. Morokuma, O. Farkas, J. B. Foresman, and D. J. Fox, Gaussian, Inc., Wallingford CT, 2016.
[91] A. Schmidpeter, K.-H. Zirzow, A. Willhalm, J. M. Holmes, R. O. Day, R. R. Holmes, *Angew. Chem. Int. Ed. Engl.* **1986**, *25*, 457–458.
[92] L. Weber, G. Dembeck, H.-G. Stammler, B. Neumann, *Eur. J. Inorg. Chem.* **1998**, 579–582.
[93] S. A. Buckler, *J. Am. Chem. Soc.* **1962**, *84*, 3093–3097.
[94] R. Gao, D. G. Ho, T. Dong, D. Khuu, N. Franco, O. Sezer, M. Selke, *Org. Lett.* **2001**, *3*, 3719–3722.
[95] J.-E. Siewert, A. Schumann, C. Hering-Junghans, *Dalton Trans.* **2021**, *50*, 15111–15117.
[96] K. H. Moock, M. H. Rock, *J. Chem. Soc. Dalton Trans.* **1993**, 2459–2463.
[97] K. Izod, P. Evans, P. G. Waddell, M. R. Probert, *Inorg. Chem.* **2016**, *55*, 10510–10522.
[98] M. R. K. Ramachandran, G. Schnakenburg, M. Majumdar, Z. Kelemen, D. Gál, L. Nyulászi, R. T. Boeré, R. K. Streubel, *Inorg. Chem.* **2022**, *61*, 4639–4646.
[99] M. R. K. Ramachandran, P. C. Brehm, G. Schnakenburg, T. Sasamori, R. T. Boeré, R. K. Streubel, *Dalton Trans.* **2023**, *52*, 7948–7956.
[100] L. M. Amrei, P. W. Dibble, R. T. Boeré, *Can. J. Chem.* **2016**, *94*, 392–400.
[101] G. Gilli, P. Gilli, *"Molecules and molecular crystals" in C. Giaccovazo et al. Fundamentals of Crystallography*, 3rd ed. Oxford University Press, Oxford, UK, p. 604.
[102] S. C. Capelli, H. B. Burgi, B. Dittrich, S. Grabowsky, D. Jayatilaka, *IUCrJ* **2014**, *1*, 361–379.
[103] O. V. Dolomanov, L. J. Bourhis, R. J. Gildea, J. A. K. Howard, H. Puschmann, *J. Appl. Crystallogr.* **2009**, *42*, 339–341.
[104] F. Neese, *WIREs Comput. Mol. Sci.* **2022**, 12, e1606.
[105] L. J. Bourhis, O. V. Dolomanov, R. J. Gildea, J. A. Howard, H. Puschmann, *Acta Crystallogr. Sect. A* **2015**, *71*, 59–75.
[106] R. I. Cooper, *Struct. Bond.* **2020**, *185*, 43–68.
[107] N. D. D. Hill, E. Lilienthal, C. O. Bender, R. T. Boeré, *J. Org. Chem.* **2022**, *87*, 16213–16229.
[108] F. Marszaukowski, R. T. Boeré, K. Wohnrath, *Cryst. Growth Des.* **2022**, *22*, 2512–2533.
[109] S. Suduweli Kondage, T. L. Roemmele, R. T. Boeré, *Synlett* **2023**, *34*, 1113–1121.
[110] R. T. Boeré, *Crystals* **2023**, *13*, 293.

Manuscript received: August 4, 2023
Revised manuscript received: August 29, 2023
Accepted manuscript online: August 30, 2023
Version of record online: September 18, 2023